Microwave, r_0 structural parameters, conformational stability and vibrational assignment of (chloromethyl)fluorosilane

Microwave, r_0 Structural Parameters, Conformational Stability and Vibrational Assignment of (Chloromethyl)fluorosilane

Gamil A. Guirgis[a], Dattatray K. Sawant[1b], Reid E. Brenner[2b], Bhushan S. Deodhar[b], Nathan A. Seifert[c], Yannick Geboes[d], Brooks H. Pate[c], Wouter A. Herrebout[d], Daniel V. Hickman[a] and James R. Durig[b*]

[a] Department of Chemistry and Biochemistry, College of Charleston, Charleston, SC 29424, USA
[b] Department of Chemistry, University of Missouri-Kansas City, Kansas City, MO 64110, USA
[c] Department of Chemistry , University of Virginia, Charlottesville, VA 22904, USA
[d] Department of Chemistry, Universitair Centrum Antwerpen, 171 Groenenborglaan, Antwerpen 2020, Belgium

[*]Corresponding author, phone: 01-816-235-6038, fax: 01 816-235-2290, email: durigj@umkc.edu
[1]Taken in part from the thesis of Dattatray K. Sawant, which will be submitted in partial fulfillment of the Ph.D. degrees.
[2]Taken in part from the thesis of Reid E. Brenner, which will be submitted in partial fulfillment of the Ph.D. degrees.

ABSTRACT: The FT-microwave spectrum (6.5 – 26 GHz) of (chloromethyl)fluorosilane, $ClCH_2$-SiH_2F has been recorded and 250 transitions for the parent species along with ^{13}C, ^{37}Cl, ^{29}Si and ^{30}Si isotopologues have been assigned for *trans* conformer. Infrared spectra (3,100 to 400 cm^{-1}) of gas, solid and the variable temperature (-60 to -100 °C) studies of the infrared spectra of the sample dissolved in xenon have been recorded. Additionally the variable temperature (-133 to -153 °C) studies of the Raman spectra of the sample dissolved in krypton have been recorded. The enthalpy difference between the *trans* and *gauche* conformers in xenon solutions has been determined to be 109 ± 15 cm^{-1} (1.47 ± 0.16 kJ mol^{-1}) and in krypton solution the enthalpy difference has been determined to be 97 ± 16 cm^{-1} (1.16 ± 0.19 kJ mol^{-1}) with the *trans* conformer as the more stable form. Approximately 46 ± 2 % of the *trans* form is present at ambient temperature. By utilizing the microwave rotational constants of five isotopologues for *trans* and the structural parameters predicted from MP2(full)/6-311+G(d,p) calculations, adjusted r_0 parameters have been obtained for *trans* conformer. The r_0 structural parameter values for the *trans* form are for the heavy atom distances (Å): Si-F = 1.608 (3); C-Cl = 1.771 (3); Si-C = 1.884 (3); and angles (°):∠FSiC = 108.9 (5); ∠ClCSi = 104.9 (5). The results are discussed and compared to the corresponding properties of some related molecules.

Key words: (chloromethyl)fluorosilane; r_0 structural parameters; *ab initio* calculations; vibrational assignments; structural parameters; conformational stability.

1. Introduction

Computational chemists determined structural parameters, conformational stability, enthalpy difference between two or more conformers and the rotational barrier heights of (halomethyl)halosilanes (XCH_2SiH_2Y where X,Y = H, F, Cl, Br and I) by using different theoretical methods. The molecular mechanics approach was used to calculate structural parameters, energies, rotational barrier heights and torsional force constants of halogenated methyl silane (XCH_2SiH_2X; X = F, Cl, Br) derivatives. The calculated energy differences between the *trans* and *gauche* conformers were observed to be small with *trans* conformer as the most stable form for (halomethyl)halosilanes, (halomethyl)dihalosilanes and (dihalomethyl)dihalosilanes.[1] However, when excess charges on the atoms were neglected the *gauche* conformer was calculated to be most stable form.[1] Density functional theory (DFT) and second order Møller-Plesset theory (MP2) were used for calculating structural parameters and energy differences between the *gauche* and *trans* conformers of (halomethyl)halosilane derivatives. According to calculations for all (halomethyl)halosilane derivatives, the *trans* conformer was predicted as the most stable form. The energy differences between the two conformers and the rotational barrier height of (halomethyl)halosilane compounds increases as the size of halogen increases.[2] Theoretical studies help to understand conformational stability, structural parameters, enthalpy differences and the rotational barrier heights of (halomethyl)halosilane.

For (chloromethyl)chlorosilane ($ClCH_2SiH_2Cl$) the *trans* to *gauche* and *gauche* to *gauche* barrier were determined to be 875 and 765 cm^{-1}. The conformational stabilities of

(chloromethyl)chlorosilane and (chloromethyl)bromosilane ($ClCH_2SiH_2Br$) were determined by utilizing variable temperature FT-IR spectra of the sample dissolved in the krypton solution whereas the conformational stability was only predicted for (chloromethyl)fluorosilane ($ClCH_2SiH_2F$).[3] For (chloromethyl)chlorosilane and (chloromethyl)bromosilane, the enthalpy difference between the two most stable conformers was determined to be 175 cm^{-1}. In a later study, the enthalpy difference for (chloromethyl)bromosilane was corrected to be 216 cm^{-1}.[4] For both molecules, the *trans* conformer was observed to be the most stable form. In the case of (chloromethyl)fluorosilane, according to theoretical calculations, the enthalpy difference between the *trans* and *gauche* conformer was expected to be 300 cm^{-1}; however, based on the intensity of the peaks the authors suggested the enthalpy difference between the two conformers should be approximately 150 cm^{-1} [5] but did not mentioned a specific value for the enthalpy difference. The vibrational assignment was reported only for the *trans* conformer of (chloromethyl)fluorosilane. To date, there is no information regarding the structural parameters and potential function of the (chloromethyl)fluorosilane. Therefore it is desirable to determine conformational stability, structural parameters and potential function of (chloromethyl)fluorosilane. This data will be useful for studying the effect of different halogens on methyl silane derivatives.

In order to determine the structural parameters, we began by obtaining FT-microwave spectral data of (chloromethyl)fluorosilane. For identifying fundamental vibrational modes of (chloromethyl)fluorosilane, the Raman spectrum of the sample dissolved in liquefied krypton, and infrared spectra of the gas, amorphous and annealed solid were investigated. For determination of the enthalpy difference between *trans* and *gauche* conformers (Fig. 1), variable temperature infrared spectra of the sample dissolved in xenon solution was investigated. The variable temperature Raman spectra were also used to determine the enthalpy difference. To

support the vibrational study, *ab initio* calculations with basis sets up to aug-cc-pVTZ as well as those with diffuse functions, i.e. 6-311+G(2df,2pd), have been carried out. Density functional theory (DFT) calculations, using the B3LYP method with the same basis sets, have also been carried out. Optimized geometries, conformational stabilities, harmonic force fields, infrared intensities, Raman activities and depolarization ratios are also calculated. The results of these spectroscopic, structural and theoretical studies of (chloromethyl)fluorosilane are reported herein and compared with other similar molecules.

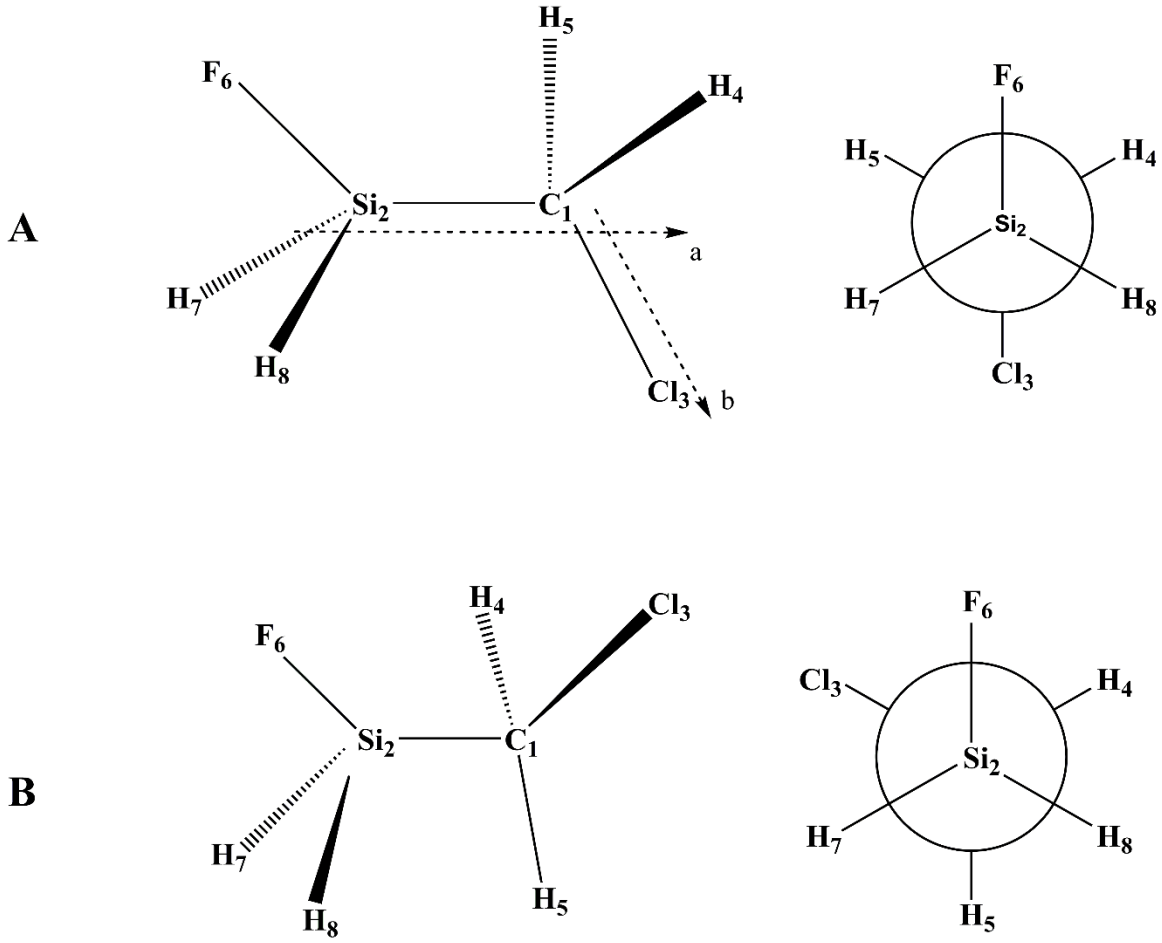

Fig. 1 Conformers of (chloromethyl)fluorosilane (A) Trans (B) Gauche.

2 Experimental methods

The sample of (chloromethyl)fluorosilane is prepared in the following steps (Scheme S1). First, (chloromethyl)trichlorosilane was treated with lithium aluminum hydride in dry dibutyl ether for 2 h at room temperature (RT). The product, (chloromethyl)silane, is brominated with boron tribromide at 0 ^{o}C for 18 h and the product, (chloromethyl)bromosilane was separated from the unreacted material as well as dibromoanalogue using trap-to-trap distillation. The purified (chloromethyl)bromosilane is fluorinated by freshly sublimed antimony trifluoride at RT for 15 min. The final product was purified twice in a low pressure low temperature sublimation column. The fraction collected at – 90 ^{o}C and 80 – 90 mTorr was used for further study.

The rotational spectrum of (chloromethyl)fluorosilane was studied using a CP-FTMW spectrometer developed at the University of Virginia, operating in the 6.5 to 18 GHz and 18 to 26 GHz ranges. The chirped pulse methods used here have been described in detail previously so only the brief details relevant to this experiment will be given.[6,7,8] The sample was prepared by balancing (chloromethyl)fluorosilane vapor with approximately 3.4 atm of Neon gas (GTS Welco) for a total sample concentration of approximately 0.2%. The resulting mixture was pulsed into the chamber at a backing pressure of approximately 1 atm for all experiments.

For the 6.5-18 GHz measurement, approximately 25,000 valve injection cycles of the sample gas, using five pulsed nozzles, were completed at 3.3 Hz to generate a directly detected, time-averaged, 50 GS/s spectrum of 250,000 molecular FIDs (approximately 2 hours of signal averaging). Additionally, the time domain resolution afforded by a 20 μs record length generates an average Doppler broadened FWHM linewidth of approximately 130 KHz (with point spacing of 24 kHz). For the 18-26 GHz measurement, approximately 29,000 valve injection cycles of the sample gas, using four pulsed nozzles, were completed at 3.3 Hz to generate a directly detected, 100 GS/s, time-averaged spectrum of 290,000 molecular FIDs. Due to the shortened Doppler decay timescale and the more stringent Nyqist sampling limits, only a 10 μs record length for

molecular FID detection was used, which affords an average Doppler broadened linewidth of 260 kHz (with a 50 kHz point spacing).

These measurements afford a frequency-domain dynamic range of approximately 1000:1, which enabled assignment of all common heavy atom single isotopologues (^{13}C, ^{37}Cl, ^{29}Si, ^{30}Si) in natural abundance. The rotational temperature for the species detected in this experiment is roughly 1.5 K. Comparison between the observed frequencies and those from a least-squares fit for the *trans* conformer of (chloromethyl)fluorosilane are listed in Table 1.

Table 1. Rotational transition frequencies (MHz) of the ground vibrational state for parent species and isotopologues of *trans* (chloromethyl)fluorosilane.

Parent species

Transitions	F″	F′	ν_{obs} (MHz)	$\Delta\nu$ [a]	Transitions	F″	F′	ν_{obs} (MHz)	$\Delta\nu$ [a]
$6_{06} \leftarrow 5_{15}$	5	4	6562.1615	-0.0027		2	2	16358.4932	0.0066
	8	7	6563.3839	-0.0017		5	5	16361.7171	0.0105
	6	5	6564.6646	-0.0036		4	3	16363.1476	0.0129
	7	6	6565.9307	-0.0037		3	3	16365.3835	0.0121
$1_{11} \leftarrow 2_{02}$	2	1	8694.4903	0.0064		4	4	16368.5498	0.0011
	3	4	8700.8563	-0.0023		2	3	16369.9544	0.0028
	1	2	8702.7288	-0.0030		3	4	16370.7923	0.0069
	3	2	8704.1223	-0.0040		5	4	16373.2415	0.0177
	2	2	8705.9263	-0.0020	$4_{13} \leftarrow 4_{04}$	4	3	16607.9081	-0.0012
	3	3	8712.3226	-0.0001		5	6	16609.9513	0.0057
	2	3	8714.1229	-0.0017		3	3	16613.8194	0.0114
$7_{07} \leftarrow 6_{16}$	8	8	10499.9914	-0.0063		6	6	16615.7114	0.0152
	6	5	10510.8108	0.0133		5	4	16617.4581	0.0081
	9	8	10511.8345	0.0125		4	4	16619.4135	0.0028
	7	6	10513.5621	0.0077		5	5	16621.5635	0.0108
	8	7	10514.6167	0.0096		4	5	16623.5189	0.0055
$3_{03} \leftarrow 2_{02}$	5	4	10831.7772	0.0101		3	4	16625.3171	0.0078
$4_{04} \leftarrow 3_{03}$	6	5	14438.5340	-0.0099		6	5	16627.3106	0.0073
$8_{08} \leftarrow 7_{17}$	7	6	14504.9142	-0.0019	$5_{14} \leftarrow 5_{05}$	4	4	16935.6907	0.0105
	10	9	14505.7671	-0.0111		7	7	16937.2289	-0.0053
	8	7	14507.7809	-0.0075		6	5	16939.1890	-0.0035
	9	8	14508.6668	-0.0035		5	5	16940.9647	-0.0118
$1_{10} \leftarrow 1_{01}$	1	1	16029.5490	-0.0076		6	6	16942.4406	0.0067
	3	3	16046.3993	-0.0101		5	6	16944.2405	0.0226
	2	1	16046.9118	-0.0058		4	5	16947.4025	0.0017
	1	2	16050.1181	-0.0128	$6_{15} \leftarrow 6_{06}$	8	8	17328.8648	0.0006
	2	3	16056.0513	-0.0122		5	5	17327.6710	0.0057
	3	2	16057.8288	-0.0090		6	6	17332.6459	-0.0123
	2	2	16067.4825	-0.0094		7	7	17333.8274	-0.0128
$2_{11} \leftarrow 2_{02}$	2	1	16164.0135	0.0044	$7_{16} \leftarrow 7_{07}$	6	6	17792.8250	-0.0165
	1	1	16165.7633	-0.0037		9	9	17793.7950	-0.0153
	3	4	16170.8793	-0.0028		8	8	17798.6565	-0.0080
	4	4	16172.6579	-0.0012	$1_{11} \leftarrow 0_{00}$	3	2	19537.539	-0.0154

Parent species

Transitions	F″	F′	ν_{obs} (MHz)	$\Delta\nu$ [a]	Transitions	F″	F′	ν_{obs} (MHz)	$\Delta\nu$ [a]
	3	2	16174.1501	0.0001		2	2	19539.3459	-0.0104
	2	2	16175.4514	-0.0021	$6_{06} \leftarrow 5_{05}$	6	5	21642.1792	0.0130
	1	2	16177.2138	0.0021	$2_{12} \leftarrow 1_{01}$	2	1	23013.8356	0.0039
	3	3	16182.3478	0.0015		3	3	23016.0721	-0.0039
	2	3	16183.6498	0.0000		1	1	23023.4761	-0.0058
	4	3	16184.1206	-0.0026		4	3	23025.7046	-0.0067
$3_{12} \leftarrow 3_{03}$	3	2	16353.9153	0.0088		3	2	23027.4979	-0.0064
	4	5	16357.0464	0.0150		2	2	23034.3996	-0.0063

[a] $\Delta\nu = \nu_{obs} - \nu_{calc}$ in MHz

^{13}C

Transitions	F″	F′	ν_{obs} (MHz)	$\Delta\nu$ [b]	Transitions	F″	F′	ν_{obs} (MHz)	$\Delta\nu$ [b]
$1_{11} \leftarrow 2_{02}$	3	4	8289.1037	1.0		3	4	15755.1326	11.8
	1	2	8290.9724	3.9		4	4	15756.8578	-7.3
	2	2	8294.1258	7.2		3	2	15758.3615	-15.4
	3	3	8300.5252	-13.2		2	2	15759.6393	-10.3
	2	3	8302.2992	0.9		1	2	15761.3941	3.4
$1_{10} \leftarrow 1_{01}$	1	1	15609.6470	11.6		3	3	15766.5513	-5.3
	3	3	15626.4729	-1.0		2	3	15767.8312	1.8
	2	1	15627.0018	-0.1		4	3	15768.3094	8.3
	1	2	15630.1593	-1.3	$3_{12} \leftarrow 3_{03}$	4	5	15947.6147	-13.2
	2	3	15636.1374	9.6		3	3	15955.9369	4.6
	3	2	15637.8715	-2.0		4	4	15959.1113	-5.8
	2	2	15647.5373	9.9	$4_{13} \leftarrow 4_{04}$	5	6	16209.2787	13.5
$2_{11} \leftarrow 2_{02}$	1	1	15749.9575	-12.7					

[b] $\Delta\nu = \nu_{obs} - \nu_{calc}$ in kHz

^{37}Cl

Transitions	F″	F′	ν_{obs} (MHz)	$\Delta\nu$ [b]	Transitions	F″	F′	ν_{obs} (MHz)	$\Delta\nu$ [b]
$1_{11} \leftarrow 2_{02}$	1	1	8917.1471	0.3		5	5	16378.8690	2.7
	2	1	8919.7204	7.5		4	3	16379.9831	2.3
	3	4	8924.7312	-1.1		3	3	16381.7459	5.5
	1	2	8926.1964	1.4		4	4	16384.2560	0.0
	3	2	8927.3059	-9.6		2	3	16385.4000	-2.6
	2	2	8928.7638	2.6		3	4	16386.0167	1.0
	3	3	8933.7957	2.9		5	4	16387.9712	6.4
	2	3	8935.2333	-4.9	$4_{13} \leftarrow 4_{04}$	4	3	16613.8094	18.8
$7_{07} \leftarrow 6_{16}$	6	5	9772.8398	1.3		5	6	16615.4118	-6.9
	9	8	9773.6483	-0.8		3	3	16618.4854	2.3
	7	6	9775.0114	-2.7		6	6	16619.9809	0.5
	8	7	9775.8453	2.2		4	4	16622.8828	-11.6
$1_{10} \leftarrow 1_{01}$	1	1	16066.3584	-5.5		5	5	16624.5776	1.6
	3	3	16079.6689	-2.3		4	5	16626.1126	-11.5
	2	1	16080.0461	-4.1		3	4	16627.5788	-8.1
	1	2	16082.6244	-4.0		6	5	16629.1471	9.5
	2	3	16087.2791	-1.1	$5_{14} \leftarrow 5_{05}$	4	4	16923.8073	13.9
	3	2	16088.7041	-1.6		7	7	16925.0295	5.3
	2	2	16096.3128	-1.8		5	5	16927.9733	10.9
$2_{11} \leftarrow 2_{02}$	2	1	16192.5467	2.4	$6_{15} \leftarrow 6_{06}$	5	5	17295.3450	-12.6

Transitions	F″	F′	ν_{obs} (MHz)	$\Delta\nu$ [b]	Transitions	F″	F′	ν_{obs} (MHz)	$\Delta\nu$ [b]
	1	1	16193.9588	-2.6		8	8	17296.2922	-2.8
	3	4	16197.9681	-1.3		6	6	17299.2650	-6.9
	4	4	16199.3961	0.0		7	7	17300.1948	-2.4
	3	2	16200.5472	-5.4	$1_{11} \leftarrow 0_{00}$	1	2	19482.7148	0.9
	2	2	16201.5902	-2.3		3	2	19483.8363	1.8
	1	2	16203.0151	5.4		2	2	19485.2803	0.2
	3	3	16207.0267	-3.0	$2_{12} \leftarrow 1_{01}$	2	1	22876.2473	-10.9
	2	3	16208.0695	-0.1		3	3	22878.0379	-11.6
	4	3	16208.4558	-0.6		1	1	22883.8797	14.5
$3_{12} \leftarrow 3_{03}$	3	2	16372.6818	6.1		4	3	22885.6434	-3.2
	4	5	16375.1566	-1.0		3	2	22887.0872	3.1
	2	2	16376.3462	8.1		2	2	22892.5284	5.7

[b] $\Delta\nu = \nu_{obs} - \nu_{calc}$ in kHz

^{29}Si

Transitions	F″	F′	ν_{obs} (MHz)	$\Delta\nu$ [b]	Transitions	F″	F′	ν_{obs} (MHz)	$\Delta\nu$ [b]
$1_{11} \leftarrow 2_{02}$	1	1	8597.1333	5.6		2	3	16064.7766	0.8
	2	1	8600.2286	-22.9		4	3	16065.2335	-2.3
	3	4	8606.6469	11.1	$3_{12} \leftarrow 3_{03}$	3	2	16235.7750	-12.3
	1	2	8608.5292	-5.5		4	5	16238.9141	7.1
	2	2	8611.6682	9.6		2	2	16240.3145	6.3
	3	3	8618.0668	3.3		5	5	16243.5395	1.6
	2	3	8619.8266	-1.2		4	3	16244.9950	5.6
$1_{10} \leftarrow 1_{01}$	1	1	15910.3035	1.7		3	3	16247.2062	-5.9
	3	3	15927.1236	-0.6		4	4	16250.3883	-1.1
	2	1	15927.6671	1.3		2	3	16251.7386	5.5
	1	2	15930.8019	-6.1		3	4	16252.6147	2.3
	2	3	15936.7762	-4.8		5	4	16255.0314	11.0
	3	2	15938.5167	1.4	$4_{13} \leftarrow 4_{04}$	3	3	16496.5832	3.2
	2	2	15948.1674	-4.6		6	6	16498.4563	-3.7
$2_{11} \leftarrow 2_{02}$	2	1	16045.2076	8.1		4	4	16502.1661	-18.1
	1	1	16046.9089	-5.2		5	5	16504.3382	-5.2
	3	4	16052.0751	5.1	$5_{14} \leftarrow 5_{05}$	5	4	16819.6889	14.4
	4	4	16053.8083	0.1		5	7	16821.2316	-7.7
	3	2	16055.3318	3.4		5	5	16825.0059	12.2
	2	2	16056.6075	1.0		5	6	16826.4439	-11.9
	1	2	16058.3173	-3.8	$1_{11} \leftarrow 0_{00}$	2	2	19406.9927	0.0
	3	3	16063.4987	1.0					

[b] $\Delta\nu = \nu_{obs} - \nu_{calc}$ in kHz

^{30}Si

Transitions	F″	F′	ν_{obs} (MHz)	$\Delta\nu$ [b]	Transitions	F″	F′	ν_{obs} (MHz)	$\Delta\nu$ [b]
$1_{11} \leftarrow 2_{02}$	1	1	8507.5118	2.2		3	3	15949.8261	0.1
	3	4	8516.9517	1.7		2	3	15951.0774	4.8
	1	2	8518.8615	-11.0		4	3	15951.5133	-5.9
	2	2	8521.9118	-3.6	$3_{12} \leftarrow 3_{03}$	3	2	16122.7712	-18.6
	3	3	8528.3465	12.6		4	5	16125.9242	13.0
	2	3	8530.0511	-1.9		2	2	16127.2528	2.1
$1_{10} \leftarrow 1_{01}$	1	1	15796.2714	1.9		5	5	16130.4937	5.9
	3	3	15813.0602	3.8		4	3	16131.9623	-8.7

Transitions	F″	F′	ν_{obs} (MHz)	$\Delta\nu$ [b]	Transitions	F″	F′	ν_{obs} (MHz)	$\Delta\nu$ [b]
	2	1	15813.6340	-0.4		3	3	16134.1829	11.7
	1	2	15816.6959	0.2		4	4	16137.3508	0.0
	2	3	15822.7106	-3.2		2	3	16138.6396	7.6
	3	2	15824.4090	5.9		3	4	16139.5368	-14.0
	2	2	15834.0493	-11.2	$5_{14} \leftarrow 5_{05}$	4	4	16708.5995	-21.7
$2_{11} \leftarrow 2_{02}$	2	1	15931.5717	-0.2		7	7	16710.1858	-3.9
	1	1	15933.2376	-3.0		5	5	16713.9489	-10.4
	4	4	15940.1471	11.7		6	6	16715.4279	-1.2
	3	2	15941.6900	1.7	$6_{15} \leftarrow 6_{06}$	6	6	17108.6745	8.5
	2	2	15942.9423	7.4		7	7	17109.8755	15.8

[b] $\Delta\nu = \nu_{obs} - \nu_{calc}$ in kHz

All final fits for all assigned species were performed using the AABS package[9] as a front end to SPFIT,[10] including all assigned values for the quartic centrifugal distortion and nuclear quadrupole hyperfine constants. For ^{13}C, ^{29}Si and ^{30}Si isotopologues, distortion and hyperfine parameters are fixed to their parent species values whereas for ^{37}Cl isotopologue distortion and hyperfine parameters are allowed to change. The experimental analysis of (chloromethyl)fluorosilane spectrum was supplemented with *ab initio* electronic structure calculations to predict rotational, centrifugal distortion and quadrupole coupling constants. All calculations were performed using the Gaussian 09 suite of programs[11] at the MP2/6-311++G(d,p) level of theory.

The mid-infrared spectrum (3,100 to 400 cm^{-1}) of the gas (Fig. 2) and solid (Fig. 3) were obtained using a Perkin-Elmer model 2,000 Fourier transform spectrometer equipped with a Ge/CsI beamsplitter and a DTGS detector. Atmospheric water vapor was removed from the spectrometer housing by purging with dry nitrogen. The theoretical resolution used to obtain the spectrum of the gas was 0.5 cm^{-1} and 128 interferograms were added and transformed with a boxcar truncation function.

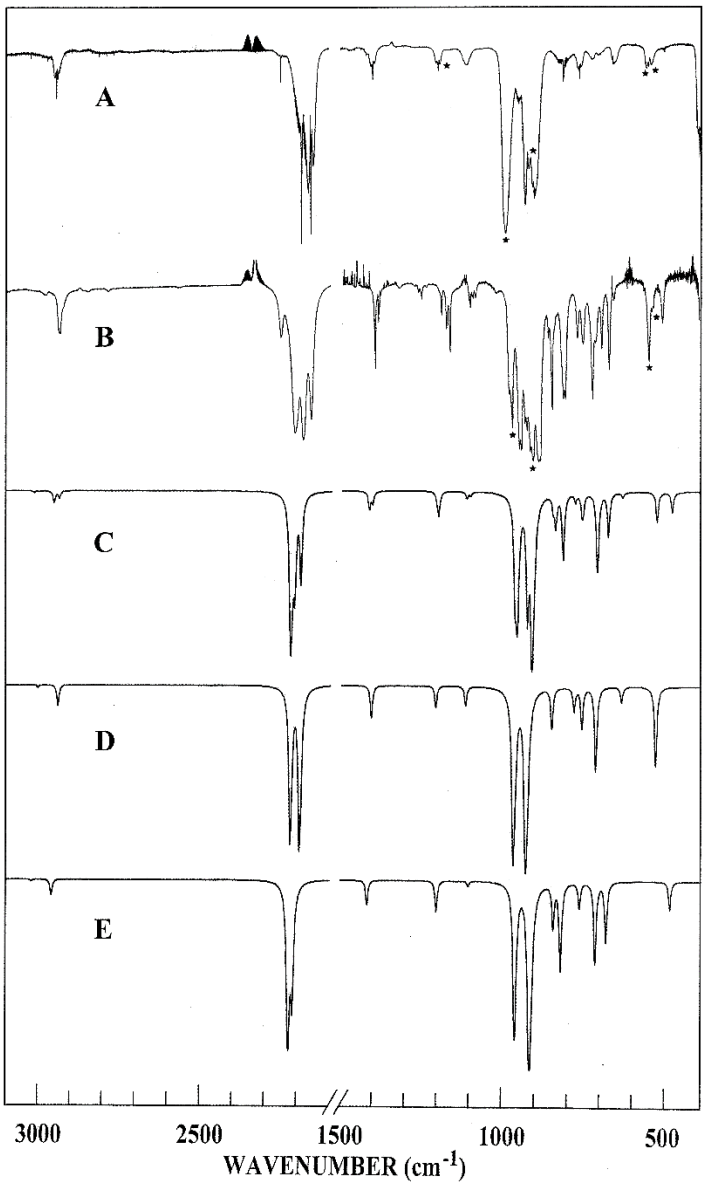

Fig. 2 Comparison of experimental and calculated infrared spectra of (chloromethyl)fluorosilane: (A) observed spectrum of gas; (B) observed spectrum of Xe solution at -70°C; (C) simulated spectrum of a mixture of *trans* and *gauche* conformers (ΔH = 109 cm^{-1}) at 25°C; (D) simulated spectrum of *gauche* conformer; (E) simulated spectrum of *trans* conformer. Peaks assigned for impurities were marked with star '★' symbol.

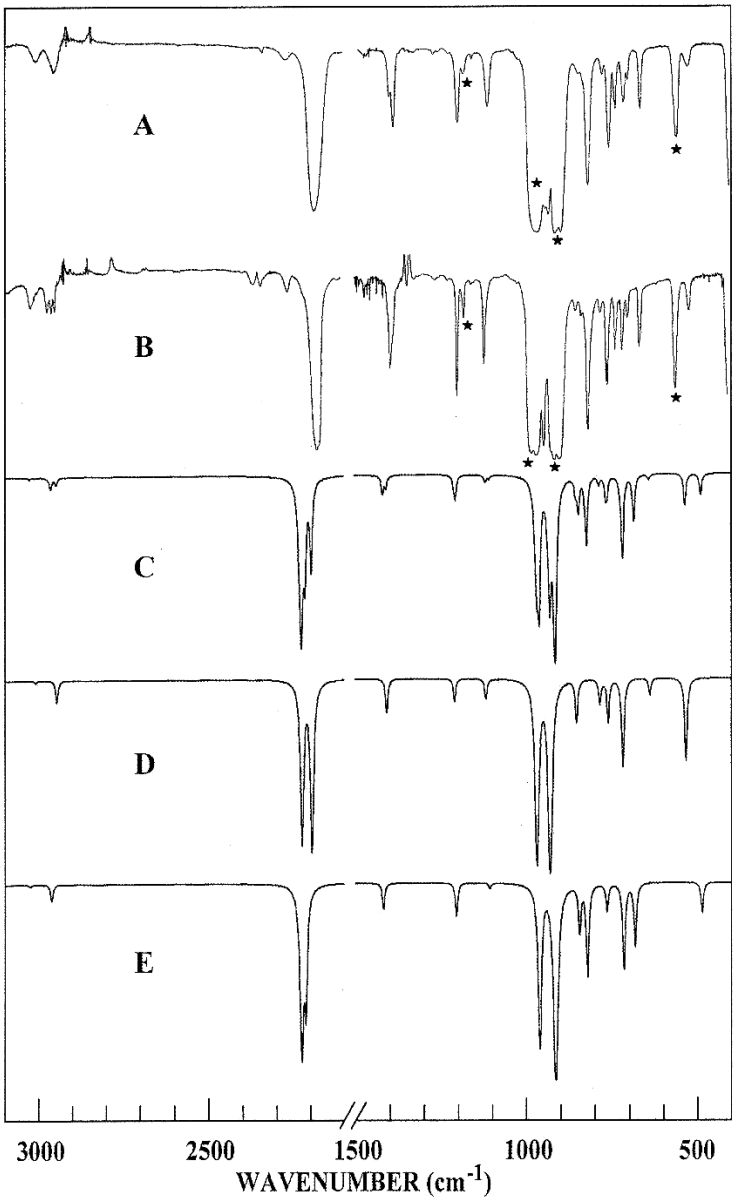

Fig. 3 Comparison of experimental and calculated infrared spectra of (chloromethyl)fluorosilane: (A) observed spectrum of amorphous solid; (B) observed spectrum of annealed solid; (C) simulated spectrum of a mixture of *trans* and *gauche* conformers (ΔH = 109 cm^{-1}) at 25°C; (D) simulated spectrum of *gauche* conformer; (E) simulated spectrum of *trans* conformer. Peaks assigned for impurities were marked with star '★' symbol.

The mid-infrared spectra (3,100 to 400 cm^{-1}) of the sample dissolved in liquefied xenon (Fig. 2) at ten different temperatures (-60 to -100 °C) were recorded on a Bruker model IFS-66 Fourier transform spectrometer equipped with a globar source, a Ge/KBr beamsplitter and a DTGS detector. In all cases, 100 interferograms were collected at 1.0 cm^{-1} resolution, averaged

and transformed with a boxcar truncation function. For these studies, a specially designed cryostat cell was used. It consists of a copper cell with a path length of 4 cm with wedged silicon windows sealed to the cell with indium gaskets. The temperature was maintained with boiling liquid nitrogen and monitored by two Pt thermoresistors. After cooling to the designated temperature, a small amount of the sample was condensed into the cell and the system was then pressurized with the noble gas, which condensed in the cell, allowing the compound to dissolve.

The Raman spectra (3050 to 400 cm^{-1}) of the sample dissolved in liquefied krypton (Fig. S1) were recorded at three different temperatures (-133 to -153 ^{o}C) on a Trivista 557 spectrometer consisting of a double f = 50 cm monochromator equipped with a 2000 lines mm^{-1} grating, a f = 70 cm spectrograph equipped with a 2400 lines mm^{-1} grating, and a back-illuminated LN2-cooled PI Acton Spec-10:2 kB/LN 2048 x 512 pixel CCD detector. For all experiments, the 514.5 nm line of a 2017-Ar S/N 1665 Spectra-Physics argon ion laser was used for Raman excitation, with the power set to 0.8 Watt. Signals related to the plasma lines were removed by using an interference filter. The frequencies were calibrated using Neon emission lines, and depending on the setup used, are expected to be accurate within 0.4 cm^{-1}. The experimental set-up used to investigate the solutions has been described before.[12,13] A home-built liquid cell equipped with four quartz windows at right angles was used to record the spectra. All of the observed bands in the Raman spectra of the sample dissolved in liquefied krypton (Fig. 4) along with their proposed assignments and depolarization values are listed in Tables 2 and 3 for the two conformers.

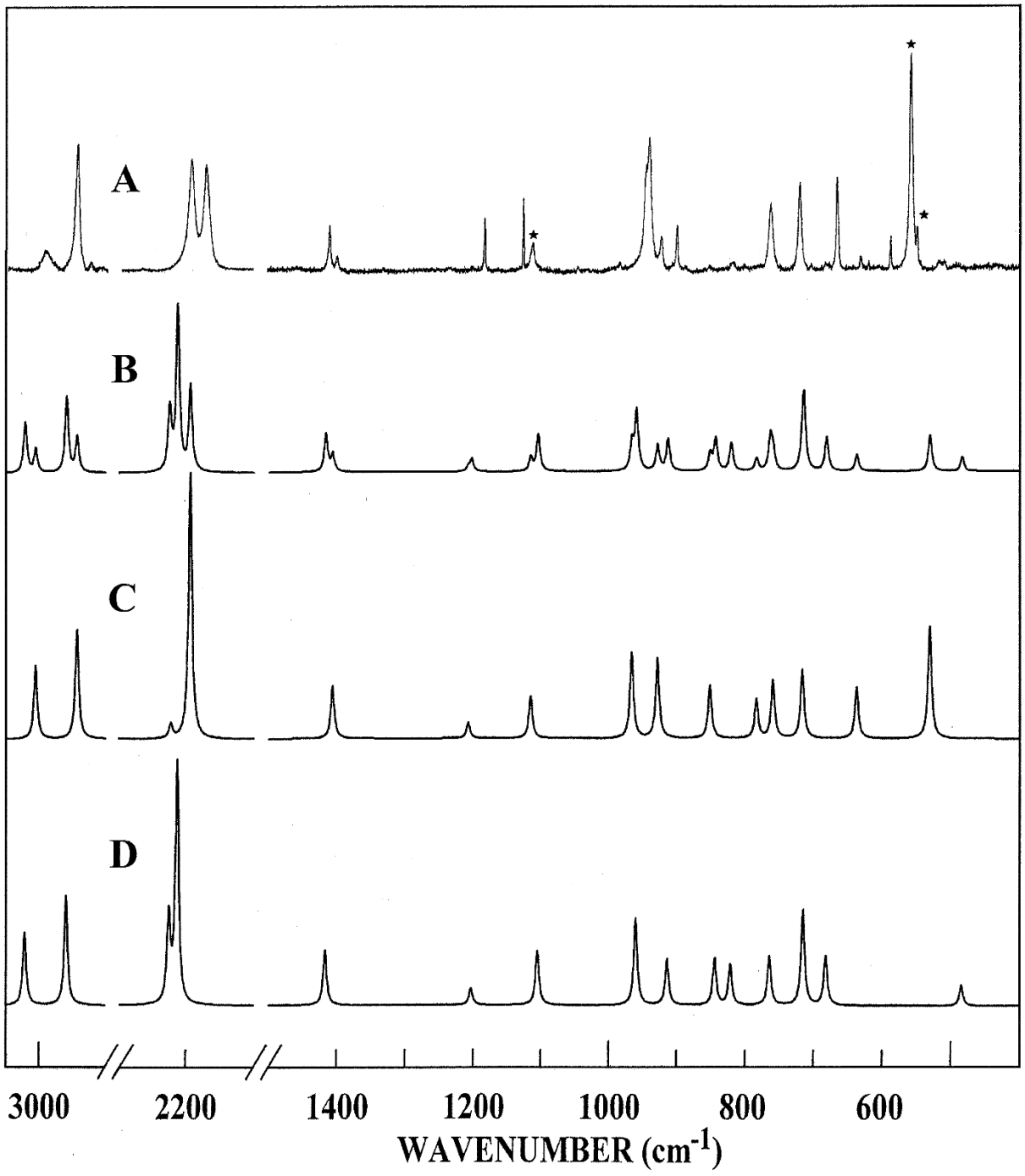

Fig. 4 Comparison of experimental and calculated Raman spectra of (chloromethyl)fluorosilane: (A) observed spectrum of sample dissolved in liquid krypton at -153°C; (B) simulated spectrum of a mixture of *trans* and *gauche* conformers (ΔH = 97 cm^{-1}) at 25°C; (C) simulated spectrum of *gauche* conformer; (D) simulated spectrum of *trans* conformer. Peaks assigned for impurities were marked with star '★' symbol.

Table 2. Calculated[a] and observed frequencies (cm^{-1}) for *trans* form of (chloromethyl)fluorosilane.

Sym. block	Vib. No.	Approx. description	*ab initio*	fixed scaled[b]	IR int.	Raman act.	dp	IR				Raman	P.E.D.[c]	Band Contour		
								gas	xenon	Solid Amorphous	Solid Annealed	Krypton		A	B	C
A′	ν_1	CH_2 symmetric stretch	3154	2959	7.0	94.1	0.10	2953	2941	2953	2956	2947	$100S_1$	72	28	-
	ν_2	SiH_2 symmetric stretch	2359	2213	84.4	128.7	0.08	2164	2161	2180	2181	2167	$100S_2$	1	99	-
	ν_3	CH_2 deformation	1511	1417	11.5	15.8	0.71	1405	1403	1400	1405	1408	$99S_3$	54	46	-
	ν_4	CH_2 wag	1282	1203	14.8	3.9	0.40	1200	1197	1199	1199	1192	$73S_4$, $25S_8$	53	47	-
	ν_5	SiH_2 deformation	1014	960	141.4	15.1	0.60	962	959	967	963	945	$97S_5$	26	74	-
	ν_6	SiH_2 wag	965	914	310.5	7.5	0.64	899	899	900	898	899	$62S_6$, $18S_7$, $10S_{10}$	92	8	-
	ν_7	Si-F stretch	891	844	22.1	6.9	0.58	847	-	844	850	848	$74S_7$, $18S_6$	10	90	-
	ν_8	C-Cl stretch	806	764	12.2	6.4	0.71	768	762	760	761	763	$60S_8$, $38S_{11}$	58	42	-
	ν_9	C-Si stretch	713	682	31.6	5.6	0.12	664	662	662	664	666	$44S_9$, $34S_8$, $10S_{10}$,	72	27	-
	ν_{10}	CSiF in-plane-bend	263	258	3.5	3.3	0.37	-	-	-	-	-	$47S_{10}$, $22S_9$, $12S_{11}$	0	100	-
	ν_{11}	SiCCl in-plane-bend	148	146	10.1	0.3	0.26	-	-	-	-	-	$44S_{11}$, $24S_{10}$, $19S_4$, $11S_6$	29	71	-
A″	ν_{12}	CH_2 antisymmetric stretch	3222	3022	0.8	65.0	0.75	2964	2983	3001	3017	2991	$100S_{12}$	-	-	100
	ν_{13}	SiH_2 antisymmetric stretch	2372	2225	172.4	45.8	0.75	2190	2186	2180	2182	2189	$100S_{13}$	-	-	100
	ν_{14}	CH_2 twist	1178	1105	2.2	11.2	0.75	-	-	-	-	-	$77S_{14}$, $21S_{16}$	-	-	100
	ν_{15}	CH_2 rock	872	821	51.4	5.8	0.75	817	815	816	813	819	$43S_{15}$, $39S_{17}$, $19S_{14}$,	-	-	100
	ν_{16}	SiH_2 twist	763	715	46.2	11.4	0.75	713	719	711	714	721	$98S_{16}$	-	-	100
	ν_{17}	SiH_2 rock	513	485	13.4	1.5	0.75	-	-	-	-	-	$59S_{17}$, $34S_{16}$,	-	-	100
	ν_{18}	torsion	86	86	6.3	1.2	0.75	-	-	-	-	-	$99S_{18}$	-	-	100

[a] MP2(full)/6-31G(d) *ab initio* calculations, scaled frequencies, infrared intensities (km/mol), Raman activities ($Å^4$/u), depolarization ratios (dp) and potential energy distributions (P.E.D.s).

[b] Scaled frequencies with scaling factors of 0.88 for CH and SiH stretches and CH deformation, 0.90 for all other modes except torsion and heavy atom bends.

[c] Symmetry coordinates with P.E.D. contribution less than 10% are omitted.

Table 3. Calculated[a] and observed frequencies (cm^{-1}) for *gauche* form of (chloromethyl)fluorosilane.

Vib. No.	Approx. description	*ab initio*	fixed scaled[b]	IR int.	Raman act.	dp	IR				Raman Krypton	P.E.D.[c]	Band Contour		
							gas	Xenon	Solid Amorphous	Solid Annealed			A	B	C
ν_{12}	CH_2 antisymmetric stretch	3204	3006	1.1	64.3	0.72	2964	2983	3001	2997	2991	$98S_{12}$	15	31	54
ν_1	CH_2 symmetric stretch	3137	2943	9.7	92.4	0.10	2949	2941	2953	2956	2947	$99S_1$	44	50	6
ν_{13}	SiH_2 antisymmetric stretch	2370	2223	139.0	7.6	0.33	2195	2186	2180	2181	2190	$69S_{13}$, $31S_2$	1	1	98
ν_2	SiH_2 symmetric stretch	2339	2194	157.5	140.5	0.15	2166	2161	2180	2181	2167	$69S_2$, $31S_{13}$	53	46	1
ν_3	CH_2 deformation	1500	1407	15.3	15.0	0.71	1399	1392	1390	1397	1398	$99S_3$,	77	7	17
ν_4	CH_2 wag	1287	1208	9.8	3.6	0.33	1200	1197	1199	1199	1192	$73S_4$, $25S_9$,	29	46	25
ν_{14}	CH_2 twist	1189	1116	8.6	8.8	0.73	1114	1107	1112	1119	1124	$74S_{14}$, $22S_{16}$	26	54	20
ν_5	SiH_2 deformation	1023	967	206.8	15.0	0.67	962	959	967	963	945	$66S_5$,$13S_7$	8	77	15
ν_6	SiH_2 wag	979	929	269.9	13.3	0.73	931	929	927	923	922	$48S_6$, $33S_5$	87	4	9
ν_7	Si-F stretch	900	852	19.7	7.9	0.63	847	855	844	850	848	$70S_7$, $19S_6$,	32	48	20
ν_8	C-Cl stretch	826	784	10.9	5.2	0.75	774	776	774	777	773	$58S_8$, $29S_{11}$	5	-	95
ν_{17}	SiH_2 rock	803	760	20.2	7.4	0.68	761	759	753	756	763	$39S_{17}$, $20S_{16}$, $11S_{15}$	51	-	49
ν_{15}	SiH_2 twist	763	717	48.3	8.2	0.72	727	728	735	734	722	$85S_{15}$	2	14	84
ν_{16}	CH_2 rock	672	638	7.3	5.3	0.35	-	-	-	-	-	$31S_{16}$, $27S_{11}$, $10S_{10}$, $10S_{17}$	86	1	13
ν_9	C-Si stretch	561	532	43.8	9.1	0.43	527	-	523	519	519	$37S_9$, $21S_{10}$, $13S_{18}$, $14S_4$	48	31	21
ν_{10}	CSiF-in-plane-bend	276	272	11.9	1.4	0.47	-	-	-	-	-	$43S_{10}$, $22S_9$, $14S_6$	71	-	28
ν_{11}	SiCCl in-plane-bend	167	167	0.1	0.6	0.24	-	-	-	-	-	$25S_{11}$, $45S_{17,}$ $24S_8$	6	1	93
ν_{18}	torsion	76	76	2.0	0.3	0.73	-	-	-	-	-	$88S_{18}$	4	95	1

[a] MP2(full)/6-31G(d) *ab initio* calculations, scaled frequencies, infrared intensities (km/mol), Raman activities ($Å^4$/u), depolarization ratios (dp) and potential energy distributions (P.E.D.s).

[b] Scaled frequencies with scaling factors of 0.88 for CH and SiH stretches and CH deformation, 0.90 for all other modes except torsion and heavy atom bends. .

[c] Symmetry coordinates with P.E.D. contribution less than 10% are omitted.

3 Theoretical methods

The *ab initio* calculations were performed with the Gaussian 03 program[14] by using Gaussian-type basis functions. The energy minima with respect to nuclear coordinates were obtained by the simultaneous relaxation of all geometric parameters by the gradient method of Pulay.[15] Several basis sets as well as the corresponding ones with diffuse functions were employed with the Møller-Plesset perturbation method[16] to the second order (MP2(full)) along with the density functional theory by the B3LYP method. The predicted conformational energy differences are listed in Table 4.

Table 4. Calculated electronic energies (hartree, E_h) and energy differences (cm^{-1}) for (chloromethyl)fluorosilane.

Basis set	MP2(full)		B3LYP	
	trans[a]	*gauche*[b]	*trans*[a]	*gauche*[b]
6-31G(d)	0.6326327	318	2.1008633	300
6-31+G(d)	0.6514445	320	2.1147702	342
6-31G(d,p)	0.6659758	307	2.1060481	299
6-31+G(d,p)	0.6843526	311	2.1197753	337
6-311G(d,p)	0.9825008	310	2.2005730	301
6-311+G(d,p)	0.9922688	322	2.2061834	361
6-311G(2d,2p)	1.0826543	345	2.2157242	295
6-311+G(2d,2p)	1.0892120	399	2.2195446	359
6-311G(2df,2pd)	1.1731938	359	2.2227718	278
6-311+G(2df,2pd)	1.1796752	385	2.226983	329
MP2(full)/aug-cc-pVTZ	1.1151651	442	2.2387781	332

[a] Energy of *trans* conformer is given as – (E + 888) E_h.
[b] Energy of *gauche* conformer is relative to *trans* form.

In order to obtain a description of the molecular motions involved in the fundamental modes of (chloromethyl)fluorosilane, a normal coordinate analysis has been carried out. The force field in Cartesian coordinates was obtained with the Gaussian 03 program at the MP2(full) level with the 6-31G(d) basis set. The internal coordinates used to calculate the **G** and **B** matrices are given in Table S1 with the atomic numbering shown in Fig. S2. By using the **B** matrix,[17] the force field in Cartesian coordinates was converted to a force field in internal coordinates. Subsequently, scaling factors of 0.88 for CH and SiH stretches and CH deformations, and 0.9 for other coordinates were applied except for the heavy atom bends and torsions, along with the geometric average of the scaling factors for the interaction force constants, to obtain the fixed scaled force field and resultant wavenumbers. A set of symmetry coordinates was used (Table S1) to determine the corresponding potential energy distributions (P.E.D.s). A comparison between the observed and calculated wavenumbers, along with the calculated infrared intensities, Raman activities, depolarization ratios and potential energy distributions for the *trans* and the *gauche* conformers are listed in Tables 2 and 3, respectively.

The vibrational spectra were predicted from the MP2(full)/6-31G(d) calculations. The predicted scaled frequencies were used together with a Lorentzian function to obtain the simulated spectra. Infrared intensities were obtained based on the dipole moment derivatives with respect to Cartesian coordinates. The derivatives were transformed with respect to normal coordinates by $(\partial\mu_u/\partial Q_i) = \sum_j (\partial\mu_u/\partial X_j)L_{ij}$, where Q_i is the i^{th} normal coordinate, X_j is the j^{th} Cartesian displacement coordinate, and L_{ij} is the transformation matrix between the Cartesian displacement coordinates and the normal coordinates. The infrared intensities were then calculated by $[(N\pi)/(3c^2)]\,[(\partial\mu_x/\partial Q_i)^2 + (\partial\mu_y/\partial Q_i)^2 + (\partial\mu_z/\partial Q_i)^2]$. Infrared spectra of the gas and the predicted infrared spectra for the pure *trans* and *gauche* conformers, as well as the mixture

of the two conformers with relative concentrations calculated for the equilibrium mixture at 25ºC by using the experimentally determined enthalpy difference are shown in Fig. 2. The predicted spectrum is in good agreement with the experimental spectrum which shows the utility of the scaled predicted frequencies and predicted intensities for supporting the vibrational assignment.

Additional support for the vibrational assignments was obtained from the simulated Raman spectra (Fig. 4). The evaluation of Raman activity by using the analytical gradient methods has been developed[18–21] and the activity S_j can be expressed as: $S_j = g_j(45\alpha_j^2 + 7\beta_j^2)$, where g_j is the degeneracy of the vibrational mode j, α_j is the derivative of the isotropic polarizability, and β_j is the anisotropic polarizability. To obtain the Raman scattering cross sections, the polarizabilities are incorporated into S_j by multiplying S_j with $(1-\rho_j)/(1+\rho_j)$ where ρ_j is the depolarization ratio of the j^{th} normal mode. The Raman scattering cross sections and calculated wavenumbers obtained from the Gaussian 03 program [14] were used together with a Lorentzian function to obtain the simulated Raman spectra. Comparison of experimental Raman spectra of sample dissolved in liquefied krypton and the predicted Raman spectra for the pure *trans* and *gauche* conformers, as well as the mixture of the two conformers with relative concentrations calculated for the equilibrium mixture at 25°C by using the experimentally determined enthalpy difference (97 cm^{-1}) are shown in Fig. 4. The spectrum of the mixture is then compared to the Raman spectra of the sample dissolved in krypton solution. The predicted spectrum is in reasonable agreement with the experimental spectrum which indicates the utility of the predicted Raman spectra for the supporting vibrational assignments.

4 Microwave results

Upon consideration for the *trans* and *gauche* conformers of (chloromethyl)fluorosilane, transitions for only *trans* conformer were detected in CP-FTMW spectrum. By utilizing MP2(full)/6-311+G(d,p) basis set the energy difference between *trans* and *gauche* conformers was predicted to be 203 cm^{-1} with *trans* as the most stable conformer (Table 4). Only 'B type' P, Q and R branch lines were observed in the microwave spectrum. All single heavy atom isotopologues for *trans* conformer were detected in natural abundance. This includes ^{13}C, ^{37}Cl, ^{29}Si and ^{30}Si isotopologues (Table 1). For *trans* form of (chloromethyl)fluorosilane, 82 transitions were fitted for the parent species with a r.m.s. error of 8.6 kHz. Similarly for ^{13}C and ^{37}Cl isotopologues, 25 and 64 transitions were fitted with a r.m.s. error of 8.5 and 6.2 kHz respectively. For the ^{29}Si and ^{30}Si isotopologues of (chloromethyl)fluorosilane, 43 and 36 transitions were fitted with a r.m.s. error of 7.6 and 8.7 kHz respectively. Overall errors between observed and calculated frequencies are small and transitions are well fitted for the *trans* conformer of (chloromethyl)fluorosilane.

Rotational constants predicted by MP2(full)/6-311+G(d,p) and B3LYP/6-311+G(d,p) basis sets and experimental rotational constants for *trans* conformer of (chloromethyl)fluorosilane are reported in Table 5. Rotational constants predicted by both methods are in good agreement with experimental rotational constants obtained for parent species and isotopologues of (chloromethyl)fluorosilane. Out of A, B and C rotational constants, 'A' rotational constants calculated by MP2(full)/6-311+G(d,p) method for the parent species and isotopologues of *trans* conformer of (chloromethyl)fluorosilane have higher values compared to experimental rotational constants whereas rotational constants calculated by B3LYP/6-311+G(d,p) method predicted lower values compared to the experimental rotational constants. B

and C rotational constant values predicted by MP2(full) and B3LYP calculations by utilizing 6-311+G(d,p) basis set are lower than experimental rotational constants. Rotational constants predicted by MP2(full)/6-311+G(d,p) basis set are more accurate than the rotational constants predicted by B3LYP/6-311+G(d,p) basis set. Experimental rotational constants obtained for normal and isotopic species enables direct structure determination of the heavy atom structure. The nuclear quadrupole coupling constants predicted by *ab initio* calculations for the parent species and ^{37}Cl isotopologues are in good agreement with the experimental values (Table 6). Additionally the quadrupole coupling constants for other isotopologues are also reported in Table 6.

Table 5. Experimental and predicted rotational constants including centrifugal distortion constants for *trans* conformer of (chloromethyl)fluorosilane.

	A (MHz)	*B* (MHz)	*C* (MHz)	Δ_J (kHz)	Δ_{Jk} (kHz)	*N*[a]
MP2(full)/6-311+G(d,p)	17910.7737	1820.5088	1703.3526	0.37661	-2.60284	
B3LYP/6-311+G(d,p)	17585.2216	1786.0668	1670.8424	0.37110	-2.61902	
Parent species	17794.2740(20)	1867.72449(64)	1743.66072(51)	0.587(10)	-1.27(18)	82
MP2(full)/6-311+G(d,p)	17511.1813	1819.4083	1698.7028	0.37292	-2.96340	
B3LYP/6-311+G(d,p)	17196.4118	1785.1156	1666.4319	0.36774	-2.93556	
^{13}C	17369.2567(60)	1866.7240(14)	1738.5789(23)	[0.587]	[-1.27]	25
MP2(full)/6-311+G(d,p)	17902.6887	1772.4038	1661.0966	0.36167	-2.53677	
B3LYP/6-311+G(d,p)	17578.0049	1738.6808	1629.2402	0.35595	-2.55441	
^{37}Cl	17783.5634(21)	1818.4850(11)	1700.57413(50)	0.512(22)	-2.40(36)	64
MP2(full)/6-311+G(d,p)	17773.8219	1814.4370	1696.7945	0.37680	-2.44118	
B3LYP/6-311+G(d,p)	17448.4666	1780.1019	1664.3857	0.37111	-2.47680	
^{29}Si	17668.485(42)	1861.662(66)	1737.164(13)	[0.587]	[-1.27]	43
MP2(full)/6-311+G(d,p)	17642.7888	1808.5470	1690.4475	0.37698	-2.29023	
B3LYP/6-311+G(d,p)	17317.4426	1774.2677	1658.0913	0.37112	-2.34100	
^{30}Si	17547.9341(44)	1855.5800(11)	1730.6916(16)	[0.587]	[-1.27]	36

[a] Number of frequencies fitted.

Table 6. Nuclear quadrupole coupling constants for parent species and isotopologues of *trans* (chloromethyl)fluorosilane.

	MP2(full)/6-311++G(d,p) Parent species	Parent species	^{13}C	MP2(full)/6-311++G(d,p) ^{37}Cl	^{37}Cl	^{29}Si	^{30}Si
3/2(χaa) (MHz)	-70. 2	-68.578(11)	-68.413(18)	-57.6	-54.2130(88)	-68.353(12)	-68.085(15)
1/4(χbb-χcc) (MHz)	-7.05	-7.8649(36)	-7.8970(60)	-8.05	-6.1742(28)	-7.9065(40)	-7.9520(54)
χab (MHz)	45.2	47.36(80)	34.9(39)	29.5	36.76(70)	49.83(95)	50.1(12)

5 Structural parameters

The microwave study of the title molecule was performed using the ^{13}C, ^{37}Cl, ^{29}Si and ^{30}Si isotopologues as well as the parent species. The results indicated that only the *trans* conformer was present with no evidence of the *gauche* conformer. The rotational constants for each isotopologue of the *trans* conformer were determined experimentally and by *ab initio* methods using MP2(full)/6-311+G(d,p) shown in Table 7. The structural parameters were determined using the MP2(full) and B3LYP method using the 6-311+G(d,p) basis set. The 15 experimentally determined rotational constants and calculated structural parameters were then used to determine the adjusted r_0 structural parameters for the *trans* conformer of (chloromethyl)fluorosilane in Table 8. The predicted r_0 structural parameters for *gauche* are also given in Table 8.

Table 7. Comparison of rotational constants (MHz) obtained from *ab initio* MP2(full)/6-311+G(d,p) predictions, experimental values from microwave spectra, and from the adjusted r_0 structural parameters for *trans* form of (chloromethyl)fluorosilane ($ClCH_2SiH_2F$).

Isotopologue	Rotational constant	MP2(full)/ 6-311+G(d,p)	Experimental	Adjusted r_0	$\|\Delta\|$
Parent species	A	17910.8	17794.3	17795.1	0.8
	B	1820.5	1867.7	1867.7	0.0
	C	1703.4	1743.7	1743.6	0.0
^{13}C	A	17511.2	17369.3	17369.3	0.0
	B	1819.4	1866.7	1866.5	0.2
	C	1698.7	1738.6	1738.4	0.2
^{37}Cl	A	17902.7	17783.6	17784.1	0.0
	B	1772.4	1818.5	1818.8	0.5
	C	1661.1	1700.6	1700.8	0.2
^{29}Si	A	17773.8	17668.5	17668.3	0.2
	B	1814.4	1861.7	1861.6	0.1
	C	1696.8	1737.2	1737.1	0.1
^{30}Si	A	17642.8	17547.9	17546.9	1.0
	B	1808.5	1855.6	1855.6	0.0
	C	1690.4	1730.7	1730.7	0.0

Table 8. Structural parameters (Å and degree), rotational constants (MHz) and dipole moment (debye) for (chloromethyl)fluorosilane.

Structural Parameters	Internal Coordinates	MP2(full)/ 6-311+G(d,p)		B3LYP/ 6-311+G(d,p)		Adjusted r_o	Predicted r_0
		Trans	*Gauche*	*Trans*	*Gauche*	*Trans*	*Gauche*
r (Si-F)	R_1	1.625	1.620	1.634	1.628	1.608 (3)	1.603
r (C-Cl)	R_2	1.790	1.786	1.822	1.817	1.771 (3)	1.767
r (Si-C)	R_3	1.875	1.873	1.885	1.883	1.884 (3)	1.888
r (C-H_4)	r_1	1.091	1.093	1.089	1.092	1.091 (2)	1.093
r (C-H_5)	r_2	1.091	1.092	1.089	1.091	1.091 (2)	1.092
r (Si-H_7)	r_3	1.467	1.467	1.477	1.477	1.469 (2)	1.469
r (Si-H_8)	r_4	1.467	1.472	1.477	1.482	1.469 (2)	1.474
∠ FSiC	θ_1	108.2	108.7	107.4	109.2	108.9 (5)	109.4
∠ ClCSi	θ_2	107.4	111.5	107.7	112.3	104.9 (5)	109.0
∠ H_4CSi	ψ_1	112.3	110.5	112.9	110.5	113.5 (5)	111.7
∠ H_5CSi	ψ_2	112.3	110.9	112.9	111.6	113.5 (5)	112.1
∠ H_7SiC	ψ_3	110.1	110.9	110.5	111.2	109.7 (5)	110.6
∠ H_8SiC	ψ_4	110.1	109.1	110.5	108.5	109.7 (5)	108.8
∠ H_4CH_5	ϕ_1	108.3	107.6	108.7	108.0	108.3 (5)	107.6
∠ H_7SiH_8	ϕ_2	112.1	112.1	112.3	112.1	112.1 (5)	112.1
∠ $ClCH_4$	σ_1	108.2	108.1	107.2	107.1	108.2 (5)	108.1
∠ $ClCH_5$	σ_2	108.2	108.1	107.2	107.1	108.2 (5)	108.1
∠ $FSiH_7$	σ_3	108.1	108.2	108.0	108.2	108.1 (5)	108.2
∠ $FSiH_8$	σ_4	108.1	107.7	108.0	107.5	108.1 (5)	107.7
τ ClCSiF	δ	180.0	65.5	180.0	67.8	180.0 (5)	65.5
A		17910.8	9285.4	17585.2	9315.0	17795.1	
B		1820.5	2295.5	1786.1	2204.6	1867.7	
C		1703.4	2017.3	1670.8	1953.8	1743.6	
$\lvert\mu_a\rvert$		0.071	0.592	0.102	0.495		
$\lvert\mu_b\rvert$		0.339	2.975	0.328	2.689		
$\lvert\mu_c\rvert$		0.000	0.289	0.000	0.297		
$\lvert\mu_t\rvert$		0.346	3.047	0.343	2.750		

We have found that good structural parameters for hydrocarbons and many substituted ones can be determined by adjusting the structural parameters obtained from the *ab initio* MP2(full)/6-311+G(d,p) calculations to fit the rotational constants obtained from microwave experimental data by using a computer program "A&M" (*Ab initio* and Microwave) developed[22] in our laboratory. In order to reduce the number of independent variables, the structural parameters are separated into sets according to their types where bond distances in the same set keep their relative ratio, and bond angles and torsional angles in the same set keep their difference in degrees. This assumption is based on the fact that errors from *ab initio* calculations are systematic. We have also recently shown[23] that *ab initio* MP2(full)/6-311+G(d,p) calculations predict the r_0 structural parameters for more than fifty carbon-hydrogen distances to better than 0.002 Å was compared to the experimentally determined values from isolated CH stretching frequencies which were compared[24] to previously determined values from earlier microwave studies. Therefore, all of the carbon-hydrogen distances can be taken from the MP2(full)/6-311+G(d,p) predicted values for (chloromethyl)fluorosilane. The same adjustment of the structural parameters using the MP2 method to get the adjusted r_0 parameters for the *trans* conformer were applied to the *gauche* conformer's structural parameters using the MP2 method to get the predicted r_0 structural parameters for the *gauche* conformer. Therefore the systematic adjustment made to the *gauche* conformer's structural parameters were the same as the adjustment for *trans* for each given bond distance and bond angle.

The internal coordinates, basis set, conformer, and adjusted parameters have all been given in Table 8. The MP2(full) and B3LYP methods are used for general comparison and to further increase accuracy of the adjusted r_0 parameters. The bond distances are given first followed by bond angles and then one torsional angle. The resulting calculated and adjusted r_0

parameters for the *trans* conformer are given in Table 8 where the heavy atom distances should be accurate to ±0.003 Å, the C-H distances accurate to ±0.002 Å, and uncertainties of angles should be within ±0.5°. The differences between experimental and adjusted rotational constants are less than 1.0 where the largest difference can be seen for the ^{30}Si isotopologue (Table 7).

Most of the structural parameters predicted by *ab initio* calculations using the MP2 method are in good agreement with the adjusted r_0 parameters for the *trans* conformer (Table 8). There are however some changes in bond distances and bond angles containing heavy atoms that are worth mentioning. Most of the calculated parameters either increased slightly or not adjusted further. The r (C-Cl) bond distance decreased from 1.790 to 1.771 Å. The r (Si-F) bond distance and ∠ ClCSi bond angle decreased from 1.625 Å to 1.608 Å and 107.4° to 104.9° respectively. Additionally there were other parameters that were adjusted by a significant amount. The r (Si-C) bond distance and ∠ $H_{4,5}$CSi bond angle increased from 1.875 Å to 1.884 Å and 112.3° to 113.5° respectively. By using the Kraitchman equation, the r (C-Cl), r (Si-C) bond distances and the ∠ ClCSi bond angle were calculated to be 1.808(9), 1.853(5) Å and 104.7(5) ° respectively. The planar moments (P_{aa}, P_{bb}, P_{cc}) obtained for all assigned species and MP2(full)/6-311++G(d,p) are reported in Table 9. The overestimation of calculated bond length and bond angles are mainly due to a calculated large P_{aa} value from MP2(full)/6-311++G(d,p) basis set calculation which is largely due to the zero point effects. A vibrationally averaged structure using anharmonic corrections would likely alleviate these issues. It might be prudent to see how use of a larger basis set compresses this bond length theoretically.

Table 9. The three planar moments (*Paa*, *Pbb*, *Pcc*) for parent species and isotopologues of *trans* (chloromethyl)fluorosilane with the *ab initio* values for parent species.

	MP2(full)/6-311+G(d,p)	Parent Species	^{13}C	^{37}Cl	^{29}Si	^{30}Si
P_{aa} (u Å^2)	273.04	266.011(15)	266.160(20)	273.338(50)	266.89(25)	267.7831(10)
P_{bb} (u Å^2)	23.65	23.8269(52)	24.525(18)	23.8438(42)	24.029(21)	24.2267(89)
P_{cc} (u Å^2)	4.566	4.5743(10)	4.5707(55)	4.57451(75)	4.5741(86)	4.5732(15)

6 Vibrational assignment

From both MP2(full) and B3LYP calculations for (chloromethyl)fluorosilane, the *trans* conformer was predicted as the most stable conformer compared to the *gauche* form (Table 4). In the microwave study, transitions were observed only for the *trans* conformer. Additionally, in the previous study there is no vibrational assignment reported for the *gauche* conformer of (chloromethyl)fluorosilane[5]. In order to determine the conformational stability and enthalpy difference between *trans* and *gauche* form of (chloromethyl)fluorosilane, it is important to make confident vibrational assignments. For this purpose, significant assistance was obtained from the *ab initio* MP2(full)/6-31G(d) calculations with two scaling factors to obtain the force constants. From these data the frequencies, infrared intensities, Raman activities, band contours and depolarization ratios were predicted (Table 2 and 3).

The *trans* conformer of (chloromethyl)fluorosilane has C_s group symmetry and vibrational modes are divided into A′ and A″ blocks whereas *gauche* conformer has C_1 group symmetry and all vibrational modes are in one block. The A′ block of the *trans* conformer has eleven vibrational modes and A″ block has seven vibrational modes. A peak observed with medium intensity at 2953 cm^{-1} is assigned for CH_2 symmetric stretch (ν_1) fundamental mode and the peak observed with high intensity at 2161 cm^{-1} is assigned for SiH_2 symmetric stretch (ν_2) fundamental mode in the infrared spectra of gaseous sample. The CH_2 deformation (ν_3) fundamental mode is predicted at 1417 cm^{-1} with medium intensity and observed at 1405 cm^{-1} in the infrared spectra of gaseous sample. The same mode (ν_3) is observed at 1408 cm^{-1} in the Raman spectra of the sample dissolved in liquid krypton. Additionally the peaks observed at 1400 cm^{-1} in the infrared spectra of amorphous solid and a shoulder peak observed at 1405 cm^{-1}

in the infrared spectra of annealed solid are assigned for the CH_2 deformation (ν_3) mode. A small intensity peak observed at 1200 cm^{-1} is assigned to the CH_2 wag (ν_4) fundamental mode. The SiH_2 deformation (ν_5) and the SiH_2 wag (ν_6) fundamental modes are assigned to peaks observed at 962 and 899 cm^{-1} respectively in the infrared spectra of sample in gaseous form. For the heavy atom stretches, the Si-F stretch (ν_7) and the C-Cl stretch (ν_8) fundamental modes are predicted at 844 and 764 cm^{-1} respectively. The modes however are observed at 847 cm^{-1} (ν_7) and 768 cm^{-1} (ν_8) respectively. The C-Si stretch (ν_9) fundamental mode is predicted at 764 cm^{-1} and observed at 664 cm^{-1}.

In the A″ block of the *trans* conformer, the CH_2 antisymmetric stretch (ν_{12}) and SiH_2 antisymmetric stretch (ν_{13}) fundamental modes are predicted at 3022 and 2225 cm^{-1}. The corresponding peaks are observed at 2964 cm^{-1} (ν_{12}) and 2190 cm^{-1} (ν_{13}) respectively. The CH_2 twist (ν_{14}) fundamental mode is predicted at 1105 cm^{-1} with low infrared intensity and medium Raman activity. However in the spectra, no peak is observed near the predicted region in the infrared and Raman spectra of the sample. The CH_2 rock (ν_{15}) fundamental mode is predicted at 821 cm^{-1} and peak observed at 817 cm^{-1} in the infrared spectra of gaseous sample. The same (ν_{15}) fundamental mode is assigned for a peak observed at 819 cm^{-1} in the Raman spectra of the sample dissolved in liquid krypton. Additionally the CH_2 rock (ν_{15}) fundamental mode is observed at 816 cm^{-1} in the infrared spectra of amorphous solid and 813 cm^{-1} in the infrared spectra of annealed solid. The peak observed at 713 cm^{-1} in the infrared spectra of gaseous sample is assigned to the SiH_2 twist (ν_{16}) fundamental mode which is predicted at 715 cm^{-1}. The same (ν_{16}) fundamental mode is observed at 719 cm^{-1} in the infrared spectra of sample dissolved

in liquid xenon, 711 cm^{-1} in infrared spectra of amorphous solid and 714 cm^{-1} in infrared spectra of annealed solid.

For the *gauche* conformer of (chloromethyl)fluorosilane, peaks observed at 2964 and 2949 cm^{-1} in the infrared spectra of the gaseous sample are assigned for the CH_2 antisymmetric stretch (ν_{12}) and CH_2 symmetric stretch (ν_1) fundamental modes respectively. Similarly, strong peaks observed at 2195 and 2166 cm^{-1} in the infrared spectra of gaseous sample are assigned for the SiH_2 antisymmetric stretch (ν_{13}) and SiH_2 symmetric stretch (ν_2) fundamental modes respectively. The CH_2 deformation (ν_3) fundamental mode is assigned to a peak observed at 1399 cm^{-1} in the infrared spectra of gaseous sample. The same (ν_3) mode is observed at 1390 cm^{-1} in the infrared spectra of amorphous solid form and 1397 cm^{-1} in the infrared spectra of annealed solid. The CH_2 wag (ν_4) fundamental mode is assigned to a low intensity peak observed at 1200 cm^{-1}. The CH_2 twist (ν_{14}) fundamental mode is assigned for a small peak observed at 1114 cm^{-1} in the infrared spectra of gaseous sample and same mode is assigned for strong peak observed at 1124 cm^{-1} in the Raman spectra of sample dissolved in liquid krypton. The SiH_2 deformation (ν_5) and the SiH_2 wag (ν_6) fundamental modes are assigned for peaks observed at 962 and 931 cm^{-1} respectively. For heavy atom stretches, the Si-F stretch (ν_7) fundamental mode is assigned to a peak observed at 847 cm^{-1} in the infrared spectra of gaseous sample. The C-Cl stretch (ν_8) fundamental mode is observed at 774 cm^{-1} in the infrared spectra of gaseous sample. A peak observed at 727 cm^{-1} in infrared spectra of gaseous sample is assigned for the SiH_2 twist (ν_{15}) fundamental mode. A peak observed at 761 cm^{-1} is assigned for the SiH_2 rock (ν_{17}) fundamental mode. The C-Si (ν_9) fundamental mode is assigned for peaks observed at 523 and 519 cm^{-1} in the infrared spectra of amorphous and annealed solid respectively.

Prominent mixing is observed in ν_9, ν_{10}, ν_{11} and ν_{15} fundamental modes which are assigned for the *trans* conformer. Similarly for the *gauche* conformer, prominent mixing is observed in ν_6, ν_9, $\nu_{10,}$ ν_{16} and ν_{17} fundamental modes. In all above mentioned fundamental modes, contribution from other vibrational modes are significant. The decomposition of (chloromethyl)fluorosilane leads to formation of hydrofluoric acid along with other unknown impurities. However the decomposition rate of (chloromethyl)fluorosilane is very slow. Peaks for impurities are observed at 544, 553, 915, 979 and 1181 cm^{-1} in all infrared and Raman spectra (Figs. 2-4). Even through the sample contains impurities, the vibrational assignments are successfully made for the *trans* and the *gauche* conformers of (chloromethyl)fluorosilane.

7. Conformational stability

In the infrared spectra of amorphous solid, peaks observed at 664, 713, 817 and 1405 cm^{-1} are specifically assigned to the *trans* conformer of (chloromethyl)fluorosilane (Fig. 3, Table 2). Similarly peaks observed at 761, 1114 and 1399 cm^{-1} are specifically assigned to the *gauche* conformer of (chloromethyl)fluorosilane (Fig. 3, Table 3). In the infrared spectra of annealed solid, intensities of peaks that are assigned to the *gauche* conformer decreased while the peak intensities for the *trans* conformer increased simultaneously. Overall for (chloromethyl)fluorosilane, the *trans* form was observed as the most stable conformer. To determine the enthalpy difference between two conformers, the sample was dissolved in liquefied xenon and krypton solutions. The IR spectra of the xenon solution and Raman spectra of the krypton solution were collected at low temperature ranges of -100 to -60°C and -153 to -133°C respectively (Figs. 2 and 4). Relatively small interactions are expected to occur between xenon and the sample but the sample can associate with itself through van der Waals interactions. However, due to the very small concentration of sample (~10^{-4} molar), self-

association is greatly reduced. Therefore, only small wavenumber shifts are anticipated for the noble gas interactions when passing from the gas phase to the liquefied xenon/krypton (Fig. 5). A significant advantage of this study is that the conformer bands are better resolved in comparison with those in the infrared spectrum of the gas.

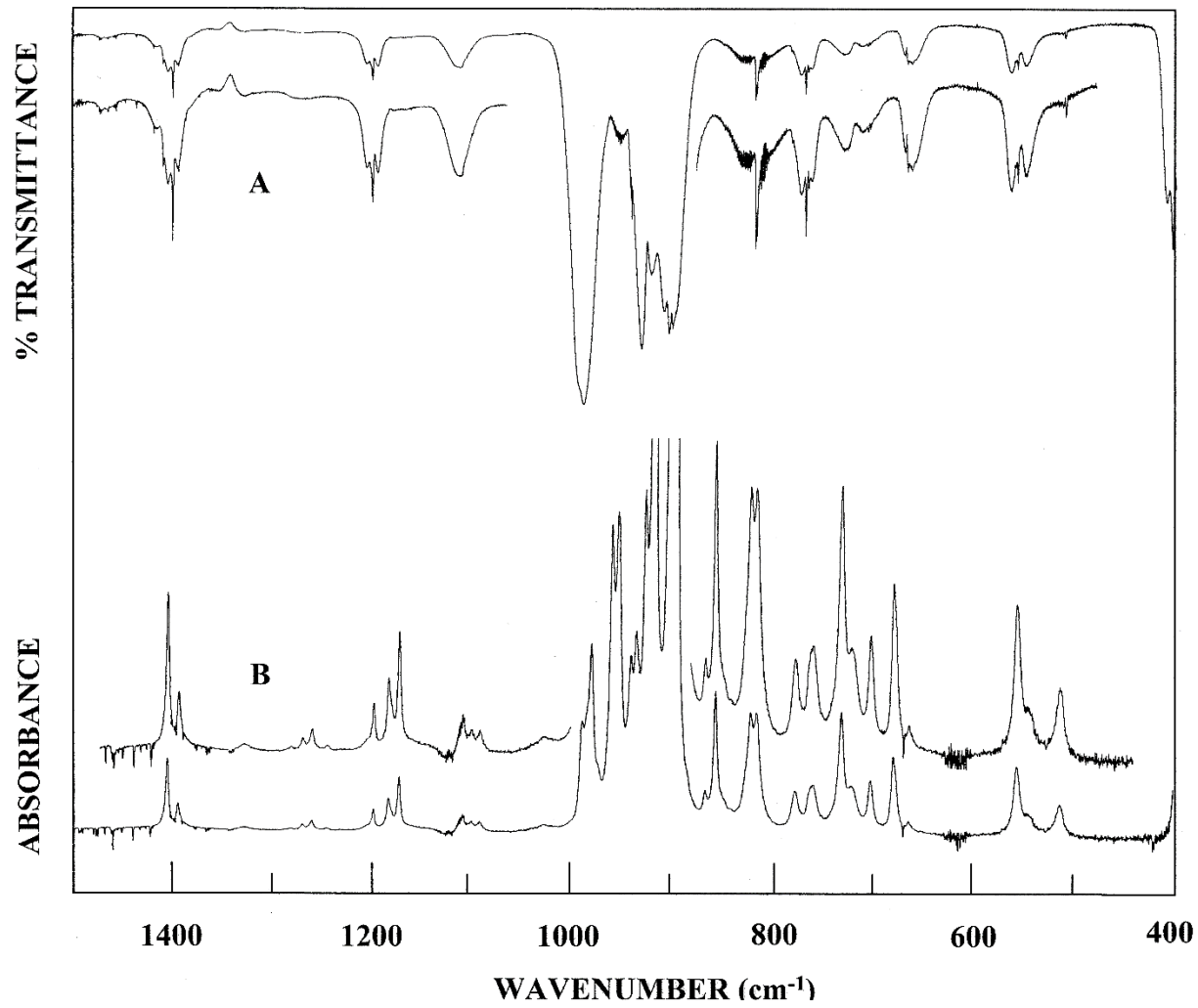

Fig. 5 Infrared spectra of (chloromethyl)fluorosilane (A) gas; (B) Xe solution at -70°C.

The vibrational assignments for the two conformers (Table 2 and 3) were used to find pairs of bands from which the enthalpy determination could be obtained. To minimize the effect

of combination and overtone bands in the enthalpy determination, it is desirable to have the lowest frequency pairs that is possible for the determination. The bands should also be sufficiently resolved so reproducible intensities can be obtained. Therefore all bands used in determining the enthalpy difference were below 1500 cm^{-1}.

The intensities of the individual bands were measured as a function of temperature and their ratios were determined (Figs. 6 and S1). By application of the van't Hoff equation $-\ln K = \Delta H/(RT) - \Delta S/R$, the enthalpy differences were determined from a plot of $-\ln K$ versus 1/T, where $\Delta H/R$ is the slope of the line and K is substituted with the appropriate intensity ratios, i.e. $I_{conf\text{-}1} / I_{conf\text{-}2}$, etc. It was assumed that ΔS and the van't Hoff factor (α) are not functions of temperature in the range studied.

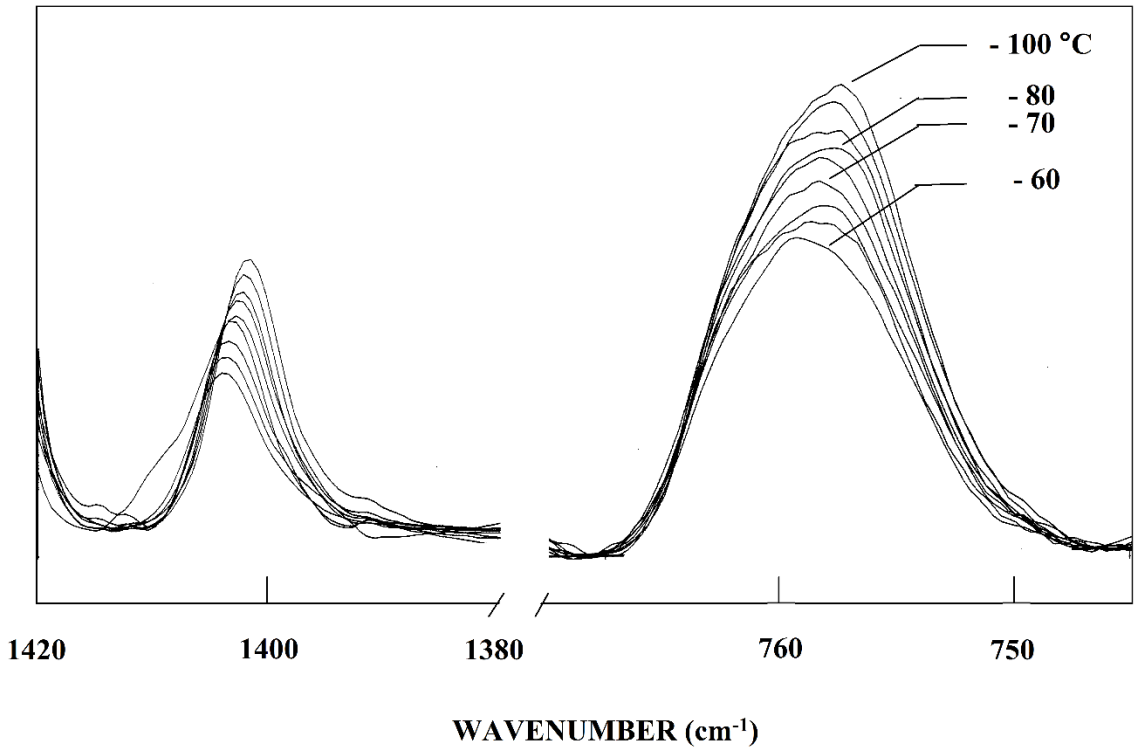

Fig. 6 Temperature (-60 to -100°C) dependent infrared spectrum of (chloromethyl)fluorosilane dissolved in liquid xenon solution.

In the IR spectra of the xenon solution, two bands at 719 cm^{-1} and 1403 cm^{-1} for the *trans* conformer and two bands at 759 cm^{-1} and 1392 cm^{-1} for the *gauche* conformer were used to determine the enthalpy difference. It is assumed that all four bands are free from impurities and have minimal mixing from other vibrations. The four bands were chosen because they were among the most resolved bands in the spectra. The intensity of each band was measured for the temperature range -100 to -60°C (Fig. 6) and recorded in Table 10. Individual enthalpy differences are determined from each band pair ratio. These enthalpy differences are then used to determine the average enthalpy ratio. The statistical average with standard deviation of one sigma was obtained by treating all the data as a single set which gives a value of 109 ± 15 cm^{-1} and indicates the *trans* conformer is more stable than the *gauche* form.

Table 10. Temperature and intensity ratios of the conformational bands of (chloromethyl)fluorosilane from the infrared spectra of the liquid xenon solution phase.

T(°C)	1/T ($\times 10^3$ K^{-1})	I_{719} / I_{759}	I_{719}/ I_{1392}	I_{1403} / I_{759}	I_{1403} / I_{1392}
–60.0	4.692	0.3092	0.9216	0.9079	2.7059
–65.0	4.804	0.3439	1.0189	0.9427	2.7925
–70.0	4.923	0.3614	1.1111	0.9458	2.9074
–75.0	5.047	0.3815	1.2000	0.9422	2.9636
–80.0	5.177	0.3736	1.1724	0.9451	2.9655
–85.0	5.315	0.3874	1.2333	0.9529	3.0333
–90.0	4.460	0.3909	1.2419	0.9645	3.0645
–95.0	5.613	0.3816	1.2344	0.9662	3.1250
–100.0	5.775	0.4038	1.3030	0.9718	3.1364
ΔH^a (cm^{-1})		129 ± 30	184 ± 36	95 ± 18	89 ± 10

[a] Average value: ΔH = 109 ± 15 cm^{-1} (1.47 ± 0.16 kJ mol^{-1}) with the *trans* conformer the more stable form and the statistical uncertainty (σ) obtained by utilizing all of the data as a single set.

The variable temperature Raman spectra (-133 to -153 °C) of the krypton solution was used to supplement the information obtained from the IR spectra of the xenon solution. Due to impurities, there were only three bands used to determine the enthalpy difference between the

conformers. The band at 819 cm^{-1} was used for the *trans* conformer and the bands at 763 and 1124 cm^{-1} were used for the *gauche*. Both band pair ratios and their enthalpies were used to obtain an average enthalpy (Table S2). The statistical average with standard deviation of one sigma was obtained by treating all the data as a single set which gives a value of 97 ± 16 cm^{-1}. This result also verifies the *trans* conformer is more stable than the *gauche* form.

The Raman spectra of the krypton solution is in good agreement with the IR spectra of the xenon solution and was used to verify the results of the conformational stability. Approximately 46 ± 2 % of the *trans* form is present at ambient temperature. Our predictions and experimentally determined energies are both in agreement that *trans* is the more stable conformer.

8. Discussion

Average and percent errors have been calculated between the predicted and the observed frequencies for the *trans* and the *gauche* conformer of (chloromethyl)fluorosilane. The *trans* and *gauche* conformers have average errors of 16.23 and 11.43 cm^{-1}, which represents percent errors of 1.13 and 0.81%, respectively. Both the average and percent errors indicate the predicted frequencies from *ab initio* calculations produced reasonably accurate results with respect to the vibrational assignments of the two conformers.

The *ab initio* calculations and experimental results indicate *trans* is the more stable conformer. The energy values of the enthalpy difference between the *trans* and *gauche* conformer significantly differ but are in qualitative agreement with the stability. This study is in good agreement with previous studies[3,4] that determined the *trans* conformer to be the most stable conformer. Previous studies of (chloromethyl)chlorosilane determined the enthalpy difference between the two conformers to be 175 cm^{-1} and 177 cm^{-1} with *trans* being more stable.[3,5] Similarly the *trans* conformer was also found to be the more stable conformer for

studies on (chloromethyl)bromosilane which determined the enthalpy difference to be 175 cm^{-1} and 216 cm^{-1}.[4,5] Collectively these studies, including this study, have a qualitative agreement in conformational stability. If the enthalpy difference for (chloromethyl)bromosilane is higher than 175 cm^{-1}, then it would confirm earlier theoretical predictions that the energy difference increases when the halogen atom on the silyl group becomes larger in size.[2]

The most probable reasons for not observing the high energy *gauche* conformer in the microwave spectra of the sample are mainly due to the conformational relaxation of (chloromethyl)fluorosilane due to supersonic expansion. The same pattern was observed for 1-hexanal where high energy conformers were also not detected.[8] Additionally the conformational relaxation can be minimized by using helium as a carrier gas but due to the experimental limitations this experiment was not carried out. Additionally the acquired spectrum contains many small peaks with hyperfine-split contaminants (or lines from decomposition products) in the regions where one would expect transitions of the *gauche* conformer to be visible. It appears there are many chlorine-containing species in the region. Given the agreement between theory and experiment for the quadrupole coupling constants of the *trans* conformer, similar agreement is expected for the predictions of gauche conformer. However, the observed spectrum is not consistent with the predicted patterns of the gauche conformer.

The adjusted r_0 structural parameters regarding the C, Cl and Si bond distances and angles from the *trans* conformer of (chloromethyl)fluorosilane will be compared to our previous study of chloromethylsilane.[25] The r (Si-C) bond distance for chloromethylsilane was determined to be 1.886 Å [25] which is almost same the determined value for (chloromethyl)fluorosilane. The r (C-Cl) bond distance for chloromethylsilane was determined to be 1.791 Å which is 0.020 Å larger than (chloromethyl)fluorosilane. Additionally the $\angle$ ClCSi bond angle decreases from

109.3° in chloromethylsilane to 104.9° for (chloromethyl)fluorosilane. It would be of interest in future studies to perform microwave studies for (chloromethyl)bromosilane and (chloromethyl)iodosilane to determine their adjusted r_0 structural parameters for comparison.

The barriers and potential function governing the asymmetric rotor motion was predicted from the MP2(full)/6-31G(d) calculations, where the energy difference was predicted to be 318 cm^{-1} between the *trans* and *gauche* conformers (Table 4). The *gauche-gauche* barrier was predicted to be 794 cm^{-1} and the *gauche* to *trans* barrier to be 1288 cm^{-1} (Fig. 7). It is possible to obtain values for four terms of the potential constants of the potential function governing the internal rotation of the (chloromethyl)fluorosilane which has the form:

$$V(\theta) = \frac{1}{2} \sum_{i=1}^{4} V_i (1-\cos i\theta)$$

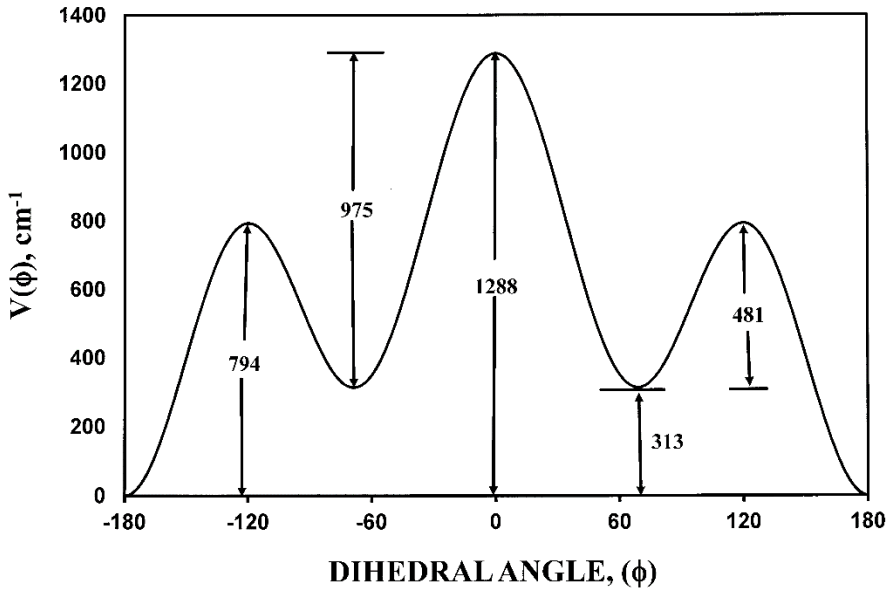

Fig. 7 Potential function (MP2(full)) governing the internal rotation of the (chloromethyl)fluorosilane from the *gauche* to the *trans* form.

The series coefficients, V_i, in the above equation, were determined by the non-linear least-squares fitting of the predicted energy differences and the torsional dihedral angles for the *gauche* (68.0°) and *trans* (180.0°) conformers and the two transition states (120.8° and -120.8°). The potential is nearly a three-fold rotation (barrier 1288 cm^{-1}) with the following values for the first four terms of the potential function: V_1 = -562.97, V_2 = -154.37, V_3 = -724.71, V_4 = 58.01 cm^{-1}. These predicted values are expected to be reasonably near the unknown experimental ones that would be obtained from the frequencies of the asymmetric torsional modes from the two conformers.

Similarly barriers and potential function were predicted for (fluoromethyl)fluorosilane, (chloromethyl)chlorosilane, (chloromethyl)bromosilane and (bromomethyl)fluorosilane from the MP2(full)/6-31G(d) calculations (Figs. S3-S6). For (fluoromethyl)fluorosilane, (chloromethyl)fluorosilane and (bromomethyl)fluorosilane (XCH_2-SiH_2F; X = F, Cl and Br) the *gauche-gauche* barriers were predicted to be 884, 794 and 1224 cm^{-1} respectively. Similarly the *gauche* to *trans* barrier was predicted to be 1531 cm^{-1} for (fluoromethyl)fluorosilane, 1288 cm^{-1} for (chloromethyl)fluorosilane and 1609 cm^{-1} for (bromomethyl)fluorosilane. The *gauche-gauche* and *gauche* to *trans* barriers were predicted low for (chloromethyl)fluorosilane compared to (fluoromethyl)fluorosilane and (bromomethyl)fluorosilane. In the comparison of (chloromethyl)fluorosilane, (chloromethyl)chlorosilane and (chloromethyl)bromosilane ($ClCH_2$-SiH_2Y; Y = F, Cl and Br) both *gauche-gauche* and *gauche* to *trans* barriers increases as the halogen atom attached to the silicon atom changed from fluorine to bromine.

Effects of different halogen (F, Cl and Br) groups on carbon and silicon atoms were studied by carrying out the Natural Population Analysis (NPA) for the *trans* and *gauche* conformers of (chloromethyl)fluorosilane, (fluoromethyl)fluorosilane,

(chloromethyl)chlorosilane, (chloromethyl)bromosilane and (bromomethyl)fluorosilane (XCH_2-SiH_2Y; X, Y = F, Cl and Br) by using MP2(full)/6-311+G(d,p) basis set (Table 11).

Table 11. Natural population analysis for (halomethyl)halosilane derivatives

XCH_2-SiH_2Y	X	C	Si	Y
Trans $ClCH_2$-SiH_2F	-0.07626	-0.82852	1.64350	-0.68214
Gauche $ClCH_2$-SiH_2F	-0.06589	-0.83823	1.65026	-0.67748
Trans FCH_2-SiH_2F	-0.43706	-0.30686	1.59438	-0.68187
Gauche FCH_2-SiH_2F	-0.43185	-0.30977	1.59348	-0.67763
Trans $ClCH_2$-SiH_2Cl	-0.07200	-0.81005	1.25122	-0.40639
Gauche $ClCH_2$-SiH_2Cl	-0.06284	-0.81548	1.24962	-0.39466
Trans $ClCH_2$-SiH_2Br	-0.07067	-0.81098	1.16688	-0.34079
Gauche $ClCH_2$-SiH_2Br	-0.06132	-0.81597	1.16221	-0.32607
Trans $BrCH_2$-SiH_2F	-0.00576	-0.92328	1.64683	-0.68276
Gauche $BrCH_2$-SiH_2F	0.00633	-0.93686	1.65776	-0.67740

Halogens attached to silicon atoms are more electronegative compared to same halogens attached to carbon atom. In the comparison of electronegativity between the *trans* and *gauche* conformer of different compounds, halogens of *trans* conformers are observed to be more electronegative compared to halogens of *gauche* conformers. Similarly carbon atoms of *gauche* conformers are more electronegative than carbon atoms of *trans* conformers. Silicon atoms of the *trans* conformer are observed to be more electropositive compared to silicon atoms of the *gauche* conformer except for (chloromethyl)fluorosilane and (bromomethyl)fluorosilane where silicon of *gauche* conformers are observed to more electropositive compared to silicon of *trans* conformers. For the *trans* and *gauche* conformer of (fluoromethyl)fluorosilane, (chloromethyl)fluorosilane and (bromomethyl)fluorosilane (XCH_2-SiH_2F; X = F, Cl and Br) as expected, electronegativity decreases from fluorine to bromine atoms but the electronegativity of carbon atom increases is observed to minimum for fluorine atom and maximum for bromine atom. The electropositivity of silicon atom increases from fluorine to bromine atoms for the *trans* and *gauche* conformer of (fluoromethyl)fluorosilane, (chloromethyl)fluorosilane and

(bromomethyl)fluorosilane. Effects of halogens attached to carbon as well as silcon atoms were studied by comparing NPA values obtained for *trans* and *gauche* conformers of (chloromethyl)fluorosilane, (chloromethyl)chlorosilane and (chloromethyl)bromosilane ($ClCH_2$-SiH_2Y; Y = F, Cl and Br). Halogens attached to silicon atoms did not have a major effect on the electronegativity of carbon atoms. For the silicon atoms however, electropositivity decreases from fluorine to bromine atoms for the *trans* and *gauche* conformers of (chloromethyl)fluorosilane, (chloromethyl)chlorosilane and (chloromethyl)bromosilane. Overall when different halogens were substituted on XCH_2-SiH_2Y (X, Y = F, Cl and Br) moiety specific trends were observed for the charge on carbon and silicon atoms of (chloromethyl)fluorosilane, (fluoromethyl)fluorosilane, (chloromethyl)chlorosilane, (chloromethyl)bromosilane and (bromomethyl)fluorosilane.

In this study the conformational stability, enthalpy difference and structural parameters of (chloromethyl)fluorosilane were determined. The effect of halogens on the carbon and silicon atoms were also studied. In the future, we are interested in studying molecules like (difluoromethyl)difluorosilane, (dichloromethyl)difluorosilane and (dibromomethyl)difluorosilane where effects of the four halogen atoms can be studied in detail.

9 Conclusion

The microwave spectrum of (chloromethyl)fluorosilane was obtained and used to determine the r_0 structural parameters. Vibrational assignments for the *trans* and *gauche* conformers were made by using the infrared spectra of the gas, solid (amorphous and annealed), and sample dissolved in liquid xenon as well as Raman spectrum of the sample dissolved in liquid krypton. The enthalpy difference and conformer stability was determined for the two conformers by using variable temperature infrared spectra dissolved in liquid xenon. The

variable temperature Raman spectra of the sample dissolved in liquid krypton confirmed the results of the infrared study of the xenon solution.

Acknowledgement

JRD acknowledges the University of Missouri–Kansas City, for a Faculty Research Grant for partial financial support of this research. GAG and DVH gratefully acknowledge the partial financial support of this study by the Camille and Henry Dreyfus Foundation by grant no. SI-14-007 and the Undergraduate Research and Creative activities at the College of Charleston.

Supporting Information available

Scheme S1. Synthesis of (chloromethyl)fluorosilane.

Table S1. Symmetry coordinates for trans conformer of (chloromethyl)fluorosilane

Table S2. Temperature and intensity ratios of the conformational bands of (chloromethyl)fluorosilane from the Raman spectra of the liquid krypton solution phase

Fig. S1 Temperature (-133 to -153 °C) dependent Raman spectrum of (chloromethyl)fluorosilane dissolved in liquid krypton solution.

Fig. S2 Internal coordinates for (chloromethyl)fluorosilane

Fig. S3 Potential function (MP2(full)) governing the internal rotation of the (fluoromethyl)fluorosilane from the trans to the gauche form.

Fig. S4 Potential function (MP2(full)) governing the internal rotation of the (chloromethyl)chlorosilane from the trans to the gauche form

Fig. S5 Potential function (MP2(full)) governing the internal rotation of the (chloromethyl)bromosilane from the trans to the gauche form.

Fig. S6 Potential function (MP2(full)) governing the internal rotation of the (bromomethyl)fluorosilane from the trans to the gauche form.

This information is available free of charge via the Internet at http://pubs.acs.org.

References:

(1) Stølevik, R.; Bakken, P. Conformational Structures, Rotational Barrier Heights and Torsional Force Constants in Diboron Tetrahalide Molecules Obtained by Molecular-Mechanics Calculations. *J. Mol. Struct. THEOCHEM* **1985**, *124*, 335–341.

(2) Bhonoah, B.; Ghoorun, A.; Abdallah, H. H.; Ramasami, P. Theoretical Study of the Gauche and Trans Conformers of $SiH_2X–CH_2X$, $SiH_2F–CH_2Y$ and $SiH_2Y–CH_2F$ (X = F, Cl, Br, I and Y = Cl, Br, I) in the Gas and Solution Phases. *J. Solution Chem.* **2011**, *40*, 430–446.

(3) Guirgis, G. A.; Pan, C.; Shen, S.; Durig, J. R. Conformational Stability of Chloromethyl Silyl Chloride from Temperature-Dependent FT-IR Spectra of Krypton Solutions. *Struct. Chem.* **2001**, *12*, 445–458.

(4) Guirgis, G. A.; Pan, C.; Durig, J. R. Spectra and Structure of Silicon-Containing Compounds. XXXIII — Raman and Infrared Spectra, Conformational Stability and Vibrational Assignment of Chloromethylsilyl Bromide. *J. Raman Spectrosc.* **2002**, *33*, 677–688.

(5) Guirgis, G. A.; Pan, C.; Shen, S.; Durig, J. R. Variable Temperature FT-IR of Krypton Solutions and Ab Initio Calculations of $ClCH_2SiH_2X$ (X=F, Cl, Br). *Asian J. Spectrosc.* **2001**, *5*, 113–122.

(6) Brown, G. G.; Dian, B. C.; Douglass, K. O.; Geyer, S. M.; Shipman, S. T.; Pate, B. H. A Broadband Fourier Transform Microwave Spectrometer Based on Chirped Pulse Excitation. *Rev. Sci. Instrum.* **2008**, *79*, 1–14.

(7) Pérez, C.; Lobsiger, S.; Seifert, N. A.; Zaleski, D. P.; Temelso, B.; Shields, G. C.; Kisiel, Z.; Pate, B. H. Broadband Fourier Transform Rotational Spectroscopy for Structure Determination: The Water Heptamer. *Chem. Phys. Lett.* **2013**, *571*, 1–15.

(8) Seifert, N. A.; Finneran, I. A.; Perez, C.; Zaleski, D. P.; Neill, J. L.; Steber, A. L.; Suenram, R. D.; Lesarri, A.; Shipman, S. T.; Pate, B. H. AUTOFIT, an Automated Fitting Tool for Broadband Rotational Spectra, and Applications to 1-Hexanal. *J. Mol. Spectrosc.* **2015**, *312*, 13–21.

(9) Kisiel, Z.; Pszczółkowski, L.; Medvedev, I. R.; Winnewisser, M.; De Lucia, F. C.; Herbst, E. Rotational Spectrum of Trans-Trans Diethyl Ether in the Ground and Three Excited Vibrational States. *J. Mol. Spectrosc.* **2005**, *233*, 231–243.

(10) Pickett, H. M. The Fitting and Prediction of Vibration-Rotation Spectra with Spin Interactions. *J. Mol. Spectrosc.* **1991**, *148*, 371–377.

(11) Frisch, M. J.; Trucks, G. W.; Schlegel, H. B.; Scuseria, G. E.; Robb, M. A.; Cheeseman, J. R.; Scalmani, G.; Barone, V.; Mennucci, B.; Petersson, G. A.; et al. Gaussian 09, Revision D.01, Gaussian, Inc., Wallingford CT, **2009**.

(12) Herrebout, W. A.; Nagels, N.; van der Veken, B. J. On the $v1^{CO2}/2v_2^{CO2}$ Resonance in the Complex of Carbon Dioxide with Dimethyl Ether. *ChemPhysChem* **2009**, *10*, 3054–3060.

(13) Michielsen, B.; Dom, J. J. J.; Veken, B. J. van der; Hesse, S.; Xue, Z.; Suhm, M. A.; Herrebout, W. A. The Complexes of Halothane with Benzene: The Temperature Dependent Direction of the Complexation Shift of the Aliphatic C–H Stretching. *Phys. Chem. Chem. Phys.* **2010**, *12*, 14034–14044.

(14) Frisch, M. J.; Trucks, G. W.; Schlegel, H. B.; Scuseria, G. E.; Robb, M. A.; Cheeseman, J. R.; Montgomery, Jr., J. A.; Vreven, T.; Kudin, K. N.; Burant, J. C.; et al. Gaussian 03, Revision C.02, Gaussian, Inc., Wallingford CT, **2004**.

(15) Pulay, P. Ab Initio Calculation of Force Constants and Equilibrium Geometries in Polyatomic Molecules. *Mol. Phys.* **1969**, *17*, 197–204.

(16) Møller, C.; Plesset, M. S. Note on an Approximation Treatment for Many-Electron Systems. *Phys. Rev.* **1934**, *46*, 618–622.

(17) Guirgis, G. A.; Zhu, X.; Yu, Z.; Durig, J. R. Raman and Infrared Spectra, Conformational Stability, Normal Coordinate Analysis, Vibrational Assignment, and Ab Initio Calculations of 3,3-Difluorobutene. *J. Phys. Chem. A* **2000**, *104*, 4383–4393.

(18) Chantry, G. W.; Anderson, A. *The Raman Effect*, 1st ed.; Anderson, A., Ed.; Maarcel Dekker Inc.: New York, **1971**.

(19) Amos, R. D. Calculation of Polarizability Derivatives Using Analytic Gradient Methods. *Chem. Phys. Lett.* **1986**, *124*, 376–381.

(20) Gaw, J. F.; Yamaguchi, Y.; Remington, R. B.; Osamura, Y.; Schaefer, H. F. Analytic Energy Third Derivatives for Open-Shell Self-Consistent-Field Wavefunctions. *Chem. Phys.* **1986**, *109*, 237–260.

(21) Polavarapu, P. L. Ab Initio Vibrational Raman and Raman Optical Activity Spectra. *J. Phys. Chem.* **1990**, *94*, 8106–8112.

(22) Van der Veken, B. J.; Herrebout, W. A.; Durig, D. T.; Zhao, W.; Durig, J. R. Conformational Stability of 3-Fluoropropene in Rare Gas Solutions from Temperature-Dependent FT-IR Spectra and Ab Initio Calculations. *J. Phys. Chem. A* **1999**, *103*, 1976–1985.

(23) Durig, J. R.; Kar, W. N.; Zheng, C.; Shen, S. Comparison of Ab Initio MP2/6-311+G(d,p) Predicted Carbon-Hydrogen Bond Distances with Experimentally Determined r_0 (C-H) Distances. *Struct. Chem.* **2004**, *15*, 149–157.

(24) McKean, D. C. New Light on the Stretching Vibrations, Lengths and Strengths of CH, SiH and GeH Bonds. *J. Mol. Struct.* **1984**, *113*, 251–266.

(25) Guirgis, G. A.; Panikar, S. S.; El Defrawy, A. M.; Kalasinsky, V. F.; Durig, J. R. Vibrational Spectra, r_0 Structural Parameters, Barriers to Internal Rotation, and Ab Initio Calculations of $ClCH_2SiH_3$, Cl_2CHSiH_3, $ClCH_2SiF_3$ and Cl_2CHSiF_3. *J. Mol. Struct.* **2009**, *922*, 93–102.